^{1}H NMR (500 MHz, $CDCl_3$) δ 1.44 (t, J = 7.00 Hz, 3H), 4.43 (q, J = 7.00 Hz, 2H), 7.44 (d, J = 8.50 Hz, 1H), 7.49–7.51 (m, 1H), 7.87, 2.35 (d, J = 2.50 Hz, 1H); ^{13}C NMR (125 MHz, $CDCl_3$) δ 14.0, 64.0, 119.0, 121.5, 129.0, 130.8, 133.2, 135.7, 153.9, 160.5; HRMS (ESI), m/z calcd for $C_{10}H_{10}Cl_2NO_3$ (MH^+) 262.0038, found 262.0031.

4.1.3. Ethyl 2-((4-chloro-3-methylphenyl)amino)-2-oxoacetate (6c)

By use of a procedure similar to that described for the preparation of compound **6b**, the aniline **4c** (3.34 g, 24.0 mmol) was converted into the title compound **6c** (4.63 g, 96% yield) as white powder.

^{1}H NMR (500 MHz, $CDCl_3$) δ 1.43 (t, J = 7.00 Hz, 3H), 2.38 (s, 3H), 4.42 (q, J = 7.00 Hz, 2H), 7.33 (d, J = 8.50 Hz, 1H), 7.43–7.46 (m, 1H), 7.51–7.54 (m, 1H), 8.82 (s, 1H); ^{13}C NMR (125 MHz, $CDCl_3$) δ 14.0, 20.2, 63.8, 118.5, 122.0, 129.7, 130.9, 134.8, 137.1, 153.8, 160.9; HRMS (ESI), m/z calcd for $C_{11}H_{13}ClNO_3$ (MH^+) 242.0578, found 242.0568.

4.1.4. Ethyl 2-((3-fluoro-4-methylphenyl)amino)-2-oxoacetate (7a)

By use of a procedure similar to that described for the preparation of compound **6b**, the aniline **5a** (3.00 g, 24.0 mmol) was converted into the title compound **7a** (4.24 g, 94% yield) as white powder.

^{1}H NMR (500 MHz, $CDCl_3$) δ 1.43 (t, J = 7.20 Hz, 3H), 2.25 (s, 3H), 4.42 (q, J = 6.80 Hz, 2H), 7.12–7.21 (m, 2H), 7.48–7.56 (m, 1H), 8.83 (s, 1H); ^{13}C NMR (125 MHz, $CDCl_3$) δ 14.2 (2C), 63.8, 107.1 (d, J = 27.5 Hz), 115.0 (d, J = 10.0 Hz), 122.3 (d, J = 17.5 Hz), 131.6 (d, J = 6.25 Hz), 135.3 (d, J = 13.8 Hz), 153.8, 160.8, 161.1 (d, J = 243.8 Hz); HRMS (ESI), m/z calcd for $C_{11}H_{13}FNO_3$ (MH^+) 226.0879, found 226.0878.

4.1.5. Ethyl 2-((3-chloro-4-methylphenyl)amino)-2-oxoacetate (7b)

By use of a procedure similar to that described for the preparation of compound **6b**, the aniline **5b** (3.40 g, 24.0 mmol) was converted into the title compound **7b** (5.19 g, 94% yield) as white powder.

^{1}H NMR (500 MHz, $CDCl_3$) δ 1.43 (t, J = 7.00 Hz, 3H), 2.35 (s, 3H), 4.42 (q, J = 7.00 Hz, 2H), 7.22 (d, J = 8.50 Hz, 1H), 7.41–7.43 (m, 1H), 7.71 (d, J = 2.00 Hz, 1H), 8.83 (s, 1H); ^{13}C NMR (125 MHz, $CDCl_3$) δ 14.0, 20.0, 63.8, 118.0, 120.3, 131.2, 133.3, 134.7, 135.0, 153.8, 160.8; HRMS (ESI), m/z calcd for $C_{11}H_{13}ClNO_3$ (MH^+) 242.0584, found 242.0573.

4.1.6. Ethyl 2-((3-bromo-4-methylphenyl)amino)-2-oxoacetate (7c)

By use of a procedure similar to that described for the preparation of compound **6b**, the aniline **5c** (4.47 g, 27.0 mmol) was converted into the title compound **7c** (6.24 g, 96% yield) as white powder.

^{1}H NMR (500 MHz, $CDCl_3$) δ 1.43 (t, J = 7.00 Hz, 3H), 2.38 (s, 3H), 4.42 (q, J = 7.00 Hz, 2H), 7.23 (t, J = 8.50 Hz, 1H), 7.48–7.53 (m, 1H), 7.83–7.90 (m, 1H), 8.80 (s, 1H); ^{13}C NMR (125 MHz, $CDCl_3$) δ 14.0, 22.4, 63.9, 118.7, 123.4, 125.0, 131.0, 135.0, 135.2, 153.7, 160.8; HRMS (ESI), m/z calcd for $C_{11}H_{13}BrNO_3$ (MH^+) 286.0079, found 286.0068.

4.1.7. N^1-(4-Chloro-3-fluorophenyl)-N^2-(2,2,6,6-tetramethylpiperidin-4-yl)oxalamide (8a)

To a solution of compound **6a** (70.0 mg, 0.286) in EtOH (2.9 mL) were added Et_3N (0.200 mL, 1.45 mmol) and 2,2,6,6-tetramethylpiperidin-4-amine (0.150 mL, 0.870 mmol). The reaction mixture was stirred for 3 h at 150 °C under microwave irradiation. After being concentrated in vacuo, the residue was extracted with $CHCl_3$, and washed with saturated $NaHCO_3$ and brine, then dried over $MgSO_4$. Concentration under reduced pressure to provide the title compound **8a** (34.6 mg, 34% yield) as white powder.

^{1}H NMR (500 MHz, $CDCl_3$) δ 0.99–1.50 (m, 15H), 1.92 (dd, J = 3.50, 9.00 Hz, 2H), 4.20–4.32 (m, 1H), 7.21–7.25 (m, 1H), 7.34–7.41 (m, 1H), 7.69–7.73 (m 1H), 9.31 (br, 1H); ^{13}C NMR (125 MHz, $CDCl_3$) δ 28.4, 34.8, 43.8, 44.5, 51.0, 108.3 (d, J = 26.3 Hz), 115.8 (d, J = 3.75 Hz), 117.1 (d, J = 17.5 Hz), 130.8, 136.2 (d, J = 8.75 Hz), 157.6, 158.1 (d, J = 247.5 Hz), 158.4; HRMS (ESI), m/z calcd for $C_{17}H_{24}ClFN_3O_2$ (MH^+) 356.1536, found 356.1548.

4.1.8. N^1-(3,4-Dichlorophenyl)-N^2-(2,2,6,6-tetramethylpiperidin-4-yl)oxalamide (8b)

By use of a procedure similar to that described for the preparation of compound **8a**, the compound **6b** (261.0 mg, 1.00 mmol) was converted into the title compound **8b** (520.0 mg, 70% yield) as white powder.

^{1}H NMR (500 MHz, $CDCl_3$) δ 1.07 (t, J = 12.0 Hz, 2H), 1.16 (s, 6H), 1.28 (s, 6H), 1.90–1.93 (m, 2H), 4.20–4.32 (m, 1H), 7.26 (m, 1H), 7.40–7.48 (m, 2H), 7.88 (s, 1H), 9.33 (s, 1H); ^{13}C NMR (125 MHz, $CDCl_3$) δ 28.5 (2C), 34.9 (2C), 43.8, 44.6 (2C), 50.9 (2C), 119.0, 121.4, 128.7, 130.8, 133.1, 135.8, 157.7, 158.5; HRMS (ESI), m/z calcd for $C_{17}H_{22}Cl_2N_3O_2$ (MH^-) 370.1095, found 370.1105.

4.1.9. N^1-(4-Chloro-3-methylphenyl)-N^2-(2,2,6,6-tetramethylpiperidin-4-yl)oxalamide (8c)

By use of a procedure similar to that described for the preparation of compound **8a**, the compound **6c** (482.0 mg, 2.00 mmol) was converted into the title compound **8c** (364.0 mg, 49% yield) as white powder.

^{1}H NMR (500 MHz, $CDCl_3$) δ 1.07 (t, J = 12.0 Hz, 2H), 1.15 (s, 6H), 1.28 (s, 6H), 1.86–1.94 (m, 2H), 4.15–4.31 (m, 1H), 7.21–7.24 (m, 1H), 7.32–7.38 (m, 2H), 7.74 (s, 1H), 9.24 (s, 1H); ^{13}C NMR (125 MHz, $CDCl_3$) δ 19.6, 28.5 (2C), 34.9 (2C), 43.7, 44.7 (2C), 50.9 (2C), 117.9, 120.2, 131.2, 133.1, 134.7, 135.1, 157.5, 158.8; HRMS (ESI), m/z calcd for $C_{18}H_{25}ClN_3O_2$ (MH^-) 350.1641, found 350.1656.

4.1.10. N^1-(3-Fluoro-4-methylphenyl)-N^2-(2,2,6,6-tetramethylpiperidin-4-yl)oxalamide (9a)

By use of a procedure similar to that described for the preparation of compound **8a**, the compound **7a** (225.0 mg, 1.00 mmol) was converted into the title compound **9a** (161.0 mg, 48% yield) as white powder.

^{1}H NMR (500 MHz, $CDCl_3$) δ 1.07 (t, J = 12.5 Hz, 2H), 1.15 (s, 6H), 1.28 (s, 6H), 1.92 (dd, J = 12.5, 3.50 Hz, 2H), 2.26 (s, 3H), 4.12–4.32 (m, 1H), 7.12–7.20 (m, 2H), 7.30–7.37 (m, 1H), 7.48–7.54 (m, 1H), 9.27 (s, 1H); ^{13}C NMR (125 MHz, $CDCl_3$) δ 14.2, 28.5 (2C), 34.9 (2C), 43.7, 44.7 (2C), 50.9 (2C), 107.1 (d, J = 26.3 Hz), 115.0, 121.8 (d, J = 17.5 Hz) 131.6, 135.4, (d, J = 15.0 Hz), 157.5, 158.8, 161.1 (d, J = 242.5 Hz); HRMS (ESI), m/z calcd for $C_{18}H_{25}FN_3O_2$ (MH^-) 334.1936, found 334.1942.

4.1.11. N^1-(3-Chloro-4-methylphenyl)-N^2-(2,2,6,6-tetramethylpiperidin-4-yl)oxalamide (9b)

By use of a procedure similar to that described for the preparation of compound **8a**, the compound **7b** (482.0 mg, 1.00 mmol) was converted into the title compound **9b** (448.0 mg, 48% yield) as white powder.

^{1}H NMR (500 MHz, $CDCl_3$) δ 1.09 (t, J = 12.5 Hz, 3H), 1.18 (s, 6H), 1.30 (s, 6H), 1.93–1.95 (m, 2H), 2.41 (s, 3H), 4.20–4.34 (m, 1H), 7.30–7.37 (m, 2H), 7.44–7.46 (m, 1H), 7.53 (d, J = 2.50 Hz, 1H), 9.25 (s, 1H); ^{13}C NMR (125 MHz, $CDCl_3$) δ 20.3, 28.5 (2C), 34.9 (2C), 43.7, 44.7 (2C), 50.9 (2C), 118.5, 122.0, 130.0, 130.7, 134.8, 137.1, 157.5, 158.8; HRMS (ESI), m/z calcd for $C_{18}H_{25}ClN_3O_2$ (MH^-) 350.1641, found 350.1636.

4.1.12. N^1-(3-Bromo-4-methylphenyl)-N^2-(2,2,6,6-tetramethylpiperidin-4-yl)oxalamide (9c)

By use of a procedure similar to that described for the preparation of compound **8a**, the compound **7c** (285.0 mg, 1.00 mmol) was converted into the title compound **9c** (157.0 mg, 40% yield) as white powder.

^{1}H NMR (500 MHz, $CDCl_3$) δ 1.07 (t, J = 12.5 Hz, 3H), 1.15 (s, 6H), 1.28 (s, 6H), 1.91 (dd, J = 8.00, 4.00 Hz, 2H), 2.38 (s, 3H), 3.70–3.75 (m, 1H), 7.22 (d, J = 8.50 Hz, 1H), 7.30–7.37 (m, 1H), 7.43–7.45 (m, 1H), 7.90 (d, J = 2.50 Hz, 1H), 9.25 (s, 1H); ^{13}C NMR (125 MHz, $CDCl_3$) δ 22.4, 28.5 (2C), 34.9 (2C), 43.7, 44.7 (2C), 50.9 (2C), 118.6, 123.4, 125.0, 131.0, 134.9 (2C), 157.5, 158.8; HRMS (ESI), m/z calcd for $C_{18}H_{25}BrN_3O_2$ (MH^-) 394.1136, found 394.1158.

4.1.13. Amine (12)

The compound **11** was prepared according to the reported procedure.[14] To a stirred solution of piridone **11** (247.8 mg, 1.05 mmol) in MeOH (2.10 mL) was added *p*-methoxybenzylamine (0.41 mL, 3.15 mmol). After being stirred at room temperature for 23 h, sodium cyanoborohydride was added and stirred at room temperature for 48 h. The reaction mixture was poured into saturated $NaHCO_3$ and extracted with EtOAc, then dried over $MgSO_4$. After concentration under reduced pressure, the residue was treated with 1 M TMS in THF (4.8 mL). The mixture was stirred at 0 °C for 14 h. Concentration under reduced pressure followed by short chromatography with $CHCl_3$/MeOH gave the PMB-protected amine. To a solution of the above amine (584.0 mg, 1.64 mmol) in CH_3CN/H_2O (13.1 mL, v:v = 2:1) was added CAN (2.74 g, 8.2 mmol). The mixture was stirred at room temperature for 14 h. The reaction mixture was diluted with 0.5 M HCl and washed with CH_2Cl_2. The water layer was alkalized and extracted with EtOAc, then dried over Na_2SO_4. Concentration under reduced pressure followed by flash chromatography over silica gel with EtOAc–EtOH (4:1) to gave the title compound **12** (175.5 mg, 71% yield) as a yellow oil.

^{1}H NMR (500 MHz, $CDCl_3$) δ 1.15–1.85 (m, 24H), 2.95–3.05 (m, 1H); ^{13}C NMR (125 MHz, $CDCl_3$) δ 22.2 (2C), 22.8 (2C), 26.2 (2C), 37.3 (2C), 42.3 (2C), 43.6 (2C), 47.0, 53.2 (2C); HRMS (ESI), m/z calcd for $C_{15}H_{29}N_2$ (MH^+) 237.2325, found 237.2321.

4.1.14. N^1-((4-Chloro-3-fluorophenyl)-N^2-(2,6-dicyclohexylpiperidin-4-yl)oxalamide (13a)

By use of a procedure similar to that described for the preparation of compound **8a**, the compound **6a** (36.8 mg, 0.150 mmol) was converted into the title compound **13a** (7.6 mg, 12% yield) as yellow powder.

^{1}H NMR (400 MHz, $CDCl_3$) δ 0.71–2.28 (m, 24H), 2.03–2.20 (m, 2H), 4.02–4.16 (m, 1H), 7.13–7.18 (m, 1H), 7.27–7.33 (m, 1H), 7.62–7.66 (m, 1H), 9.25 (br, 1H); ^{13}C NMR (125 MHz, $CDCl_3$) δ 14.1, 22.0 (2C), 22.6 (2C), 25.8 (2C), 29.3, 29.7 (2C), 31.9, 70.5, 108.3 (d, J = 26.3 Hz), 115.8, 117.1 (d, J = 18.8 Hz), 130.8, 136.2 (d, J = 10.0 Hz), 157.6, 158.1 (d, J = 247.5 Hz), 158.6; HRMS (ESI), m/z calcd for $C_{23}H_{32}ClFN_3O_2$ (MH^+) 436.2162, found 436.2156.

4.1.15. N^1-(4-Chlorophenyl)-N^2-(2,6-dicyclohexylpiperidin-4-yl)oxalamide (13b)

By use of a procedure similar to that described for the preparation of compound **8a**, the compound **6b** (31.3 mg, 0.120 mmol) was converted into the title compound **13b** (28.0 mg, 52% yield) as white powder.

^{1}H NMR (400 MHz, $CDCl_3$) δ 0.96 (t, J = 12.5 Hz, 2H), 1.10–1.84 (br, 20H), 2.05–2.19 (m, 2H), 4.08–4.21 (m, 1H), 7.23–7.33 (br, 1H), 7.39–7.46 (m, 2H), 7.88 (t, J = 1.00 Hz, 1H), 9.34 (s, 1H); ^{13}C NMR (125 MHz, $CDCl_3$) δ 14.1, 22.1 (2C), 22.7 (2C), 26.1 (2C), 31.6, 37.2 (2C), 42.6, 43.0, 43.6, 52.6 (2C), 119.0, 121.4, 128.7, 130.8, 133.1, 135.8, 157.7, 158.5; HRMS (ESI), m/z calcd for $C_{23}H_{32}Cl_2N_3O_2$ (MH^+) 452.1872, found 452.1865.

4.1.16. N^1-((4-Chloro-3-methylphenyl)-N^2-(2,6-dicyclohexylpiperidin-4-yl)oxalamide (13c)

By use of a procedure similar to that described for the preparation of compound **8a**, the compound **6c** (121.0 mg, 0.500 mmol) was converted into the title compound **13c** (15.1 mg, 7% yield) as white powder.

^{1}H NMR (500 MHz, $CDCl_3$) δ 0.87–1.88 (br, 22H), 2.09–2.20 (m, 2H), 2.38 (s, 3H), 4.09–4.22 (m, 1H), 7.32–7.33 (m, 1H), 7.41–7.43 (m, 1H), 7.51 (d, J = 2.00 Hz, 1H), 7.73 (m, 1H), 9.24 (s, 1H); ^{13}C NMR (125 MHz, $CDCl_3$) δ 20.2, 22.1 (2C), 22.7 (2C), 26.0 (2C), 29.7, 37.0, 42.3 (2C), 42.8 (2C), 43.4, 52.9 (2C), 118.4, 122.0, 130.0, 130.6, 134.8, 137.1, 157.5, 158.9; HRMS (ESI), m/z calcd for $C_{24}H_{35}ClN_3O_2$ (MH^+) 430.2267, found 430.2264.

4.1.17. N^1-(3-Fluoro-4-methylphenyl)-N^2-(2,6-dicyclohexylpiperidin-4-yl)oxalamide (14a)

By use of a procedure similar to that described for the preparation of compound **8a**, the compound **7a** (225.0 mg, 1.00 mmol) was converted into the title compound **14a** (27.5 mg, 7% yield) as white powder.

^{1}H NMR (500 MHz, $CDCl_3$) δ 0.971 (t, J = 12.5 Hz, 2H), 1.18–1.86 (m, 20H), 2.13–2.16 (m, 2H), 2.26 (s, 3H), 4.09–4.21 (m, 1H), 7.13–7.18 (m, 2H), 7.33 (d, J = 8.00 Hz, 1H), 7.50–7.53 (m, 1H), 9.27 (s, 1H); ^{13}C NMR (125 MHz, $CDCl_3$) δ 14.2, 22.2 (2C), 22.8 (2C), 26.1 (2C), 37.2 (2C), 42.2 (2C), 43.3 (2C), 43.5, 52.6 (m, 2C), 107.0 (d, J = 27.5 Hz), 115.0 (d, J = 3.75 Hz), 121.8 (d, J = 17.5 Hz), 131.6 (d, J = 6.25 Hz), 135.4 (d, J = 10.0 Hz), 157.5, 158.9, 161.3 (d, J = 242.5 Hz); HRMS (ESI), m/z calcd for $C_{24}H_{33}FN_3O_2$ (MH^-) 414.2554, found 414.2562.

4.1.18. N^1-(3-Chloro-4-methylphenyl)-N^2-(2,6-dicyclohexylpiperidin-4-yl)oxalamide (14b)

By use of a procedure similar to that described for the preparation of compound **8a**, the compound **7b** (120.5 mg, 0.500 mmol) was converted into the title compound **14b** (12.9 mg, 6% yield) as white powder.

^{1}H NMR (500 MHz, $CDCl_3$) δ 0.973 (t, J = 12.5 Hz, 2H), 1.18–1.86 (br, 20H), 2.11–2.19 (m, 2H), 2.35 (s, 3H), 4.09–4.21 (m, 1H), 7.20–7.22 (m, 1H), 7.30–7.32 (m, 1H), 7.35–7.37 (d, J = 2.50 Hz, 1H), 7.73 (m, 1H), 9.22 (s, 1H); ^{13}C NMR (125 MHz, $CDCl_3$) δ 19.6, 22.1 (2C), 22.7 (2C), 26.0 (2C), 29.7, 37.0, 42.1 (2C), 42.7 (2C), 43.2, 53.3 (2C), 118.0, 120.3, 131.2, 133.0, 134.7, 135.1, 157.5, 158.8; HRMS (ESI), m/z calcd for $C_{24}H_{33}ClN_3O_2$ (MH^+) 430.2267, found 430.2257.

4.1.19. N^1-(3-Bromo-4-methylphenyl)-N^2-(2,6-dicyclohexylpiperidin-4-yl)oxalamide (14c)

By use of a procedure similar to that described for the preparation of compound **8a**, the compound **7c** (142.0 mg, 0.500 mmol) was converted into the title compound **14c** (11.5 mg, 5% yield) as white powder.

^{1}H NMR (500 MHz, $CDCl_3$) δ 0.67–2.07 (br, 22H), 2.28 (br, 2H), 2.38 (s, 3H), 4.09–4.21 (m, 1H), 7.22 (d, J = 8.00 Hz, 1H), 7.28–7.38 (br, 1H), 7.43 (dd, J = 4.50, 2.50 Hz, 1H), 7.90 (d, J = 2.50 Hz, 1H), 9.21 (s, 1H); ^{13}C NMR (125 MHz, $CDCl_3$) δ 14.1, 22.1 (2C), 22.4 (2C), 22.7 (2C), 25.9, 30.0, 31.6, 36.9 (2C), 42.7 (3C), 52.7, 52.9, 118.6, 123.4, 125.0, 131.0, 134.9, 135.1, 157.4, 158.8; HRMS (ESI), m/z calcd for $C_{24}H_{33}BrN_3O_2$ (MH^+) 474.1762, found 474.1746.

4.2. Antiviral assay and cytotoxicity assay

Anti-HIV activity and cytotoxicity measurements in PM1/CCR5 cells (Yoshimura et al., 2010) were based on viability of cells that

had been infected or not infected with 100 TCID50 of an R5 primary isolate YTA48P exposed to various concentrations of the test compound. After the PM1/CCR5 cells were incubated at 37 °C for 7 days. The 50% inhibitory concentration (IC_{50}) values and the 50% cytotoxic concentration (CC_{50}) were then determined using the Cell Counting Kit-8 assay (Dojindo Laboratories). All assays were performed in duplicate or triplicate.

4.3. FACS analysis

JR-FL (R5, Sub B) chronically infected PM1 cells were pre-incubated with 0.5 μg/mL of sCD4 or 100 μM of a CD4 mimic for 15 min, and then incubated with an anti-HIV-1 mAb, 4C11, at 4 °C for 15 min. The cells were washed with PBS, and fluorescein isothiocyanate (FITC)-conjugated mouse anti-human IgG antibody was used for antibody-staining. Flow cytometry data for the binding of 4C11 (green lines) to the Env-expressing cell surface in the presence of a CD4 mimic are shown among gated PM1 cells along with a control antibody (anti-human CD19: black lines). Data are representative of the results from a minimum of two independent experiments. The number at the bottom of each graph shows the mean fluorescence intensity (MFI) of the antibody 4C11.

4.4. Molecular modeling

Dockings of compounds **3** and **13a** were performed using Molecular Operating Environment modeling package (MOE 2008. 10, Canada), into the crystal structure of gp120 (PDB, entry 3TGS).

Acknowledgements

This work was supported in part by Grant-in-Aid for Scientific Research from the Ministry of Education, Culture, Sports, Science, and Technology of Japan, and Health and Labour Sciences Research Grants from Japanese Ministry of Health, Labor, and Welfare. We are grateful to Professor Yoshio Hayashi and Dr. Fumika Yakushiji, Tokyo University of Pharmacy and Life Sciences for their assistance in the molecular modelings.

Supplementary data

Supplementary data (NMR charts of compounds) associated with this article can be found, in the online version, at http://dx.doi.org/10.1016/j.bmc.2013.02.041.

References and notes

1. Chan, D. C.; Kim, P. S. *Cell* **1998**, *93*, 681.
2. (a) Kadow, J.; Wang, H.-G.; Lin, P.-F. *Curr. Opin. Investig. Dugs* **2006**, *7*, 721; (b) Repik, A.; Clapham, P. R. *Structure* **2008**, *16*, 1603.
3. Holz-Smith, S.; Sun, I. C.; Jin, L.; Matthews, T. J.; Lee, K. H.; Chen, C. H. *Antimicrob. Agents Chemother.* **2001**, *45*, 60.
4. Lin, P.-F.; Blair, W.; Wang, T.; Spicer, T.; Guo, Q.; Zhou, N.; Gong, Y.-F.; Wang, H.-F. H.; Rose, R.; Yamanaka, G.; Robinson, B.; Li, C.-B.; Fridell, R.; Deminie, C.; Demers, G.; Yang, Z.; Zadjura, L.; Meanwell, N.; Colonno, R. *Proc. Natl. Acad. Sci. U.S.A.* **2003**, *100*, 11013.
5. Zhao, Q.; Ma, L.; Jiang, S.; Lu, H.; Liu, S.; He, Y.; Strick, N.; Neamati, N.; Debnath, A. K. *Virology* **2005**, *339*, 213.
6. (a) Madani, N.; Schön, A.; Princiotto, A. M.; LaLonde, J. M.; Courter, J. R.; Soeta, T.; Ng, D.; Wang, L.; Brower, E. T.; Xiang, S.-H.; Do Kwon, Y.; Huang, C.-C.; Wyatt, R.; Kwong, P. D.; Freire, E.; Smith, A. B., III; Sodroski, J. *Structure* **2008**, *16*, 1689; (b) LaLonde, J. M.; Elban, M. A.; Courter, J. R.; Sugawara, A.; Soeta, T.; Madani, N.; Princiotto, A. M.; Kwon, Y. D.; Kwong, P. D.; Schön, A.; Freire, E.; Sodroski, J.; Smith, A. B., III *Bioorg. Med. Chem. Lett.* **2011**, *20*, 354; (c) LaLonde, J. M.; Kwon, Y. D.; Jones, D. M.; Sun, A. W.; Courter, J. R.; Soeta, T.; Kobayashi, T.; Princiotto, A. M.; Wu, X.; Schön, A.; Freire, E.; Kwong, P. D.; Mascola, J. R.; Sodroski, J.; Madani, N.; Smith, A. B., III *J. Med. Chem.* **2012**, *55*, 4382.
7. Curreli, F.; Choudhury, S.; Pyatkin, I.; Zagorodnikov, V. P.; Bulay, A. K.; Altieri, A.; Kwon, Y. D.; Kwon, P. D.; Debnath, A. K. *J. Med. Chem.* **2012**, *55*, 4764.
8. (a) Yamada, Y.; Ochiai, C.; Yoshimura, K.; Tanaka, T.; Ohashi, N.; Narumi, T.; Nomura, W.; Harada, S.; Matsushita, S.; Tamamura, H. *Bioorg. Med. Chem. Lett.* **2010**, *20*, 354; (b) Narumi, T.; Ochiai, C.; Yoshimura, K.; Harada, S.; Tanaka, T.; Nomura, W.; Arai, H.; Ozaki, T.; Ohashi, N.; Matsushita, S.; Tamamura, H. *Bioorg. Med. Chem. Lett.* **2010**, *20*, 5853; (c) Narumi, T.; Arai, H.; Yoshimura, K.; Harada, S.; Nomura, W.; Matsushita, S.; Tamamura, H. *Bioorg. Med. Chem.* **2011**, *19*, 6735.
9. (a) Schön, A.; Madani, N.; Klein, J. C.; Hubicki, A.; Ng, D.; Yang, X.; Smith, A. B., III; Sodroski, J.; Freire, E. *Biochemistry* **2006**, *45*, 10973; (b) Schön, A.; Lam, S. Y.; Freire, E. *Future Med. Chem.* **2011**, *3*, 1129.
10. Yoshimura, K.; Harada, S.; Shibata, J.; Hatada, M.; Yamada, Y.; Ochiai, C.; Tamamura, H.; Matsushita, S. *J. Virol.* **2010**, *84*, 7558.
11. Kwon, Y. D.; Finzi, A.; Wu, X.; Dogo-Isonagie, C.; Lee, L. K.; Moore, L. R.; Schmidt, S. D.; Stuckey, J.; Yang, Y.; Zhou, T.; Zhu, J.; Vicic, D. A.; Debnath, A. K.; Shapiro, L.; Bewley, C. A.; Mascola, J. R.; Sodroski, J. G.; Kwong, P. D. *Proc. Natl. Acad. Sci. U.S.A.* **2012**, *109*, 5663.
12. (a) Kwong, P. D.; Wyatt, R.; Robinson, J.; Sweet, R. W.; Sodroski, J.; Hendrickson, W. A. *Nature* **1998**, *393*, 648; (b) Kwong, P. D.; Wyatt, R.; Mcajeed, S.; Robinson, J.; Sweet, R. W.; Sodroski, J.; Hendrickson, W. A. *Structure* **2000**, *8*, 1329.
13. McFarland, C.; Vicic, D. A.; Debnath, A. K. *Synthesis* **2006**, 807.
14. Sakai, K.; Yamada, K.; Yamasaki, T.; Kinoshita, Y.; Mito, F.; Utsumi, H. *Tetrahedron* **2010**, *66*, 2311.

Vaccine 28 (2010) 5377–5385

Contents lists available at ScienceDirect

Vaccine

journal homepage: www.elsevier.com/locate/vaccine

Evaluation of the immune response and protective effects of rhesus macaques vaccinated with biodegradable nanoparticles carrying gp120 of human immunodeficiency virus

Ai Himeno[a], Takami Akagi[b,d], Tomofumi Uto[c,d], Xin Wang[c,d], Masanori Baba[c,d], Kentaro Ibuki[a], Megumi Matsuyama[a], Mariko Horiike[a], Tatsuhiko Igarashi[a], Tomoyuki Miura[a,d,*], Mitsuru Akashi[b,d,**]

[a] Laboratory of Primate Model, Experimental Research Center for Infectious Diseases, Institute for Virus Research, Kyoto University, 53 Shogoinkawaramachi, Sakyo-ku, Kyoto 606-8507, Japan

[b] Department of Applied Chemistry, Graduate School of Engineering, Osaka University, 2-1 Yamadaoka, Suita, Osaka 565-0871, Japan

[c] Division of Antiviral Chemotherapy, Center for Chronic Viral Diseases, Graduate School of Medical and Dental Sciences, Kagoshima University, 8-35-1 Sakuragaoka, Kagoshima 890-8544, Japan

[d] Japan Science and Technology Agency (JST), Core Research for Evolutional Science and Technology (CREST), Saitama 332-0012, Japan

ARTICLE INFO

Article history:
Received 26 January 2010
Received in revised form 6 April 2010
Accepted 15 April 2010
Available online 14 May 2010

Keywords:
HIV vaccine
Biodegradable nanoparticles
Adjuvant

ABSTRACT

We previously reported that biodegradable amphiphilic poly(γ-glutamic acid) nanoparticles (NPs) carrying the recombinant gp120 env protein of the human immunodeficiency virus type 1 (HIV-1) were efficiently taken up by dendritic cells, and induced strong $CD8^+$ T cell responses against the gp120 in mice. To evaluate gp120-carrying NPs (gp120-NPs) as a vaccine candidate for HIV-1 infection, we vaccinated rhesus macaques with these gp120-NPs and examined the immune response and protective efficacy against a challenge inoculation of simian and human immunodeficiency chimeric virus (SHIV). We found that gp120-NP vaccination induced stronger responses for both gp120-specific cellular and humoral immunity than gp120-alone vaccination. After the challenge inoculation with SHIV, however, the peak value of viral RNA in the peripheral blood was higher in the vaccinated groups, especially the gp120-NP vaccinated group, than naive control group. Higher value of viral load was also maintained in gp120-NP vaccinated group. Furthermore, $CD4^+$ T cells from the peripheral blood decreased more in the vaccinated groups than the control group. Thus, induced immune responses against gp120 enclosed in NPs were not effective for protection but, conversely enhanced the infection, although the gp120-NPs showed a stronger induction of immune responses against the vaccinated antigen in rhesus macaques. These results support the importance of determining immune correlate of protective immunity for vaccine development against HIV-1 infection.

1. Introduction

The development of a human immunodeficiency virus type 1 (HIV-1) vaccine is much needed to prevent the continuing spread of the acquired immunodeficiency syndrome (AIDS) pandemic across the world [1]. The use of highly active antiretroviral therapy (HAART) has achieved a reduced death rate due to AIDS. HAART can efficiently suppress virus replication in HIV-1-infected individuals [2]. However, HAART is expensive, and the complete eradication of the virus from infected patients by HAART does not seem possible, suggesting the necessity for long-term treatment. Moreover, the side effects and emergence of drug resistant viruses limit the long-term application of HAART [3]. Thus, an effective, safe and affordable HIV-1 vaccine with prophylactic/therapeutic effects is the most desirable for the eradication of HIV-1 infection.

Vaccination to induce an adaptive immune response is expected for a broad range of infectious diseases. Traditional vaccines are mainly composed of live attenuated viruses or whole inactivated pathogens, and these vaccines often cause many unwanted side effects [4]. With recent advances in biotechnology, new vaccine strategies have been developed using part of the pathogen, such as recombinant/synthetic proteins or peptides, or DNA encoding for these proteins. Subunit vaccines are generally very safe, with well-defined components. However, these antigens are often

* Corresponding author at: Laboratory of Primate Model, Experimental Research Center for Infectious Diseases, Institute for Virus Research, Kyoto University, 53 Shogoinkawaramachi, Sakyo-ku, Kyoto 606-8507, Japan. Tel.: +81 75 751 3984; fax: +81 75 761 9335.

** Corresponding author at: Department of Applied Chemistry, Graduate School of Engineering, Osaka University, 2-1 Yamadaoka, Suita 565-0871, Japan. Tel.: +81 6 6879 7356; fax: +81 6 6879 7359.

E-mail addresses: tmiura@virus.kyoto-u.ac.jp (T. Miura), akashi@chem.eng.osaka-u.ac.jp (M. Akashi).

0264-410X/$ – see front matter © 2010 Elsevier Ltd. All rights reserved.
doi:10.1016/j.vaccine.2010.04.110

poorly immunogenic, and thus require the use of adjuvants or vaccine delivery systems to induce adequate immunity [5–7]. Particulate adjuvants (e.g. micro/nanoparticles, emulsions, ISCOMS, liposomes, virosomes and virus-like particles) have been widely investigated in HIV vaccine delivery systems [8]. Antigen uptake by antigen presenting cells (APCs) is enhanced by the association of these antigens with nano-sized particles. The adjuvant effect of the nanoparticles appears to be largely a consequence of their uptake into the APCs. Dendritic cells (DCs) are highly specialized APCs that can activate naive T cells, and hence initiate primary immune responses. Therefore, the active delivery of antigens to DCs is an important factor for the development of effective vaccines [9,10].

Vaccines to prevent HIV infection have focused on the induction of virus-specific neutralizing antibodies and cytotoxic T lymphocyte (CTL) responses. An important role of neutralizing antibodies for HIV-1 *env* has been demonstrated by the passive transfer of these neutralizing antibodies in animal models. The passive transfer of various human monoclonal antibodies can protect against viral challenge [11–13]. However, it should be noted that for the protection of viral transmission, a high-titer and an enormous quantity of antibodies are needed. Similarly, HIV-1-specific CTL responses have also been associated with the control of HIV-1 infection. The importance of CTL for HIV-1 infection is suggested by the inverse correlation between anti-HIV-1 CTL responses and the virus load in humans [14,15]. In addition, the depletion of $CD8^+$ T cells through the infusion of anti-CD8 antibodies decreases the control of viremia in infected macaques [16,17]. Therefore, recent vaccine approaches have focused on eliciting CTL responses [18]. To solve the problem of the poor immunogenicity of HIV-1 *env*, several candidate adjuvants and delivery systems are currently being investigated in rhesus macaques [19–22]. In fact, the first phase III trial performed using the HIV-1 gp120-based vaccine candidate AIDSVAX from VaxGen was a failure [23]. Varying degrees of protection have been demonstrated in a number of vaccine trials employing the use of a pathogenic simian immunodeficiency virus (SIV) or a chimeric simian/human immunodeficiency virus (SHIV) as the challenge virus [24].

In previous studies, we demonstrated that intranasal immunization with inactivated HIV- or SHIV-capturing polystyrene nanospheres (HIV-NS or SHIV-NS) could induce vaginal anti-HIV-1 gp120 IgA and IgG antibodies in mice [25–27] and macaques, and that SHIV-NS-immunized macaques exhibited partial protection when vaginally and systemically challenged with pathogenic viruses [28]. These results clearly indicated that HIV-1-capturing nanospheres are useful as adjuvant carriers for a prophylactic vaccine against HIV-1 infection. However, both biodegradability and biocompatibility of the adjuvant carriers are required for medical use. Therefore, the development of biodegradable nanoparticles is indispensable for clinical applications [29]. To that end, we have recently prepared protein-loaded biodegradable nanoparticles composed of hydrophobically modified poly(γ-glutamic acid) (γ-PGA) [30–33]. γ-PGA is a naturally occurring water-soluble, biodegradable, edible and non-toxic poly(amino acid)s that is synthesized by certain strains of *Bacillus*. γ-PGA hydrophobic derivatives (γ-hPGA) formed 200 nm-sized nanoparticles (NPs) in water. These protein-encapsulated γ-hPGA NPs were efficiently taken up by immature mouse DCs. These γ-hPGA NPs also had adjuvant activity for DC maturation. Thus, γ-hPGA NPs have significant potential as an antigen carrier and as an adjuvant for DCs [34,35]. Moreover, immunization with HIV-1 gp120- or p24-encapsulated γ-hPGA NPs strongly induced antigen-specific cellular immunity in mice [35–37]. These results suggest that HIV-1-related antigen-carrying γ-hPGA NPs provide a novel delivery system, and function as an adjuvant for vaccination against HIV-1 infection.

In this study, we evaluated the immune responses in macaques after intranasal and subcutaneous immunization with HIV-1 gp120-carrying γ-hPGA NPs (gp120-NPs). Moreover, to determine whether the vaccination by gp120-NPs can enhance the protective effect against pathogenic viruses, the macaques were intravenously challenged with SHIV-KU-2. Here we report the use of nanoparticles as HIV-1 vaccine adjuvants. Our results demonstrated that gp120-NPs have great potential for the induction of HIV-1 gp120-specific cellular and humoral immunity. However, the macaques immunized with gp120-NPs had an augmented viral load. These results may be helpful for the design of HIV-1 vaccines.

2. Materials and methods

2.1. Nanoparticles (NPs)

γ-PGA (number-average molecular weight, $M_n = 3.8 \times 10^5$) was kindly provided by Meiji Seika Co., Ltd., Tokyo, Japan. The synthetic procedures for the γ-hPGA NPs consisting of γ-PGA conjugated with L-phenylalanine ethylester (γ-PGA-*graft*-Phe) and protein-carrying γ-hPGA NPs have been described previously [35,36]. The mean diameter of the γ-hPGA NPs in aqueous solution was measured by a dynamic light scattering (DLS) method using a Zetasizer Nano ZS (Malvern Instruments, UK). The diameter of the NPs was about 200 nm.

2.2. Preparation of gp120-encapsulated γ-hPGA NPs for intranasal vaccination

Recombinant HIV-1 III_B envelope glycoprotein gp120 (Immuno Diagnostics, Woburn, MA) was chosen for the immunization experiments, and encapsulated into the γ-hPGA NPs (gp120-NPs). To prepare the gp120-encapsulated γ-hPGA NP, γ-PGA-*graft*-Phe (10 mg/ml in DMSO) was added to the same volume (500 μl) of 500 μg/ml recombinant gp120 to yield a translucent solution. The resulting solution was centrifuged at 14,000 × *g* for 15 min, repeatedly rinsed to remove the organic solvents, and prepared to a final particle concentration of 20 mg/ml. The gp120 loading content into the NPs was measured by the Lowry method, as previously described [35]. The amount of encapsulated gp120 into the NPs was 10 μg per mg NP.

2.3. Preparation of gp120-surface immobilized γ-hPGA NPs for subcutaneous vaccination

To prepare the gp120-immobilized γ-hPGA NPs, the carboxyl group of the γ-hPGA NPs (10 mg/ml) was first activated by water-soluble carbodiimide (1 mg/ml) for 20 min. The NPs (5 mg/ml) obtained by centrifugation (14,000 × *g* for 15 min) were suspended in 125 μg/ml gp120, and the mixture was incubated at 4 °C for 24 h. After the reaction, the centrifuged NPs were washed twice with PBS. The resulting solution was prepared to a final particle concentration of 20 mg/ml. The amount of gp120 immobilized onto the NPs was 10 μg per mg NP.

2.4. Animals

Nine rhesus macaques (*Macaca mulatta*) of the Indian origin, which spread in Japan, were used in this study. All macaques were serologically negative for simian immunodeficiency virus (SIV) and simian T cell lymphotropic virus type 1. The macaques were housed in P3 level isolators throughout the experimental period. All experiments were carried out in accordance with regulations approved by the Institutional Animal Care and Use Committee of the Institute for virus Research, Kyoto University.

2.5. Vaccination of macaques

Prior to immunization, the macaques were anesthetized by an intramuscular injection of ketamine chloride. Nine macaques were divided into three groups. Three macaques in the gp120-NP group (MM471, MM472 and MM473) were immunized with gp120-carring γ-hPGA NPs, gp120-alone group (MM471, MM472 and MM473) were immunized with gp120 only, and the 3 macaques in the PBS group (MM474, MM475 and MM476) were immunized with phosphate buffered saline (PBS) as a naive control. Each of three macaques was intranasally immunized at 0, 4, and 8 weeks. At each immunization, 0.5 ml of the inoculum (containing 100 μg of gp120 protein encapsulated into or not into 10 mg of NP) was slowly dripped using a pipette tip into both nasal cavities. In addition, these macaques received subcutaneous injections in close proximity to the axillary lymph nodes at 12 and 16 weeks with 1.5 ml of the inoculum containing 300 μg of gp120 immobilized onto or not onto 30 mg of NP.

2.6. Challenge inoculation to macaques

SHIV KU-2 was used in the experiments. SHIV KU-2 is a polyclonal chimeric SHIV generated by in vivo passage of SHIV-4, containing the envelope gene of HIV-1 HXBc2 [38]. The SHIV-KU-2 virus stock for the challenge experiments was produced by culture in rhesus macaque peripheral blood mononuclear cells (PBMCs), and stored in liquid nitrogen until use. The 50% tissue culture infectious dose ($TCID_{50}$) of the virus stock was determined by culture in M8166 cells. At 4 weeks after the last immunization, all nine macaques were intravenously challenged with SHIV-KU-2. For the intravenous challenge, macaques were anesthetized, and then 1×10^5 $TCID_{50}$ of the virus inoculum was used. Blood samples were periodically collected from all macaques. The PBMCs were separated from ACD-A blood by Percoll density centrifugation.

2.7. Quantitative analysis of anti-HIV-1 gp120 IgG and IgA antibodies

HIV-1 gp120-specific IgG and IgA antibody levels in the plasma were measured by an ELISA method. A 96-well microplate (Nunc-Immuno™ Modules, Maxisorp™, Nalga-Nunc, Rochester, NY) was coated with recombinant HIV-1 III_B gp120 (Immuno Diagnostics) at a concentration of 1 μg/ml in 0.1 M Na_2CO_3–$NaHCO_3$ buffer (pH 9.6). The plate was left over night at 4 °C, washed with washing buffer (containing 0.15 M NaCl and 0.05% Tween 20), and treated with a blocking buffer (1% BSA, 1% skim milk in washing buffer) for 2 h at room temperature. To measure the IgG and IgA antibodies, the plasma was 100-fold diluted with blocking buffer, and applied to the plate. The plate was the incubated overnight at 4 °C. After washing with washing buffer, peroxidase-conjugated goat anti-monkey IgG or IgA (Kirkegaard & Perry Laboratories, Gaithersburg, MD) was added to the plate and incubated for 2 h at room temperature. The plate was then washed, and treated with *O*-phenylenediamine dehydrochloride (OPD, Wako Pure Chemical, Osaka, Japan) for 5 min and stopped with 2N H_2SO_4. The specific absorbances were read at 490/690 nm with a microplate reader. The titers of anti-HIV1/2 antibodies in the plasma of all macaques after challenge with SHIV-KU-2 were measured by the particle agglutination (PA) method (Genedia HIV-1/2 mix PA kit, Fujirebio Inc., Tokyo, Japan) following the manufacturer's recommendations.

2.8. Antigen specific proliferation assay

PBMCs from the vaccinated macaques were cultured in triplicate in a 96-well plate (2×10^5 cells/well) with 200 μl of RPMI 1640 medium in the presence of 0.5 μg recombinant HIV-1 III_B gp120 (Immuno Diagnostics) or 1 μg SIV_{mac251} p27 purified native protein (Advanced Biotechnologies, Inc., Columbia, MD) for 72 h. Next, the antigen specific proliferations were measured by BrdU incorporation into the stimulated PBMCs using a cell proliferation ELISA kit (Roche Diagnostic CmbH, Mannheim, Germany) following the manufacturer's recommendations. The stimulation index (SI) for cell activity was calculated using the following formula: stimulation index (SI) = (OD stimulated − blank)/(OD non-stimulated − blank). A SI value above 2.5 was considered as 'antigen-specific' stimulation. Concanavalin A (Con A) was used as a polyclonal stimulator positive control.

2.9. IFN-γ ELISPOT assay

An enzyme-linked immunospot (ELISPOT) assay was performed by stimulating unfractionated PBMCs with recombinant HIV-1 III_B gp120 (Immuno Diagnostics) or SIV_{mac251} p27 purified native protein (Advanced Biotechnologies). MultiScreen 96-Well Plates (Millipore Corporation, Bedford, MA) were coated overnight (100 μl/well) at 37 °C with diluted monoclonal antibody GZ-4 (MABTECH Inc., Mariemont, OH). The plates were then washed 3 times with PBS (−) containing 0.25% Tween 20 (PBS/0.25% Tween 20). The PBMCs were plated in triplicate at 5×10^5/well in 200 μl with either medium alone, 0.5 μg HIV-1 gp120 or 1 μg SIV_{mac251} p27. Following a 72 h incubation at 37 °C, the plates were washed 3 times with PBS/0.25% Tween 20 and incubated for 4 h at 37 °C with a 1:1000 dilution of biotinylated monoclonal antibody 7-B6-1 (MABTECH Inc). Following 3 washes with PBS/0.25% Tween 20, the plates were incubated for 2 h at room temperature with a 1:1000 dilution of streptavidin-alkaline phosphatase (MABTECH Inc). The plate was developed with a BCIP:NBT:0.1 M Tris buffer solution (1:1:10) mixture (Kirkegaard & Perry Laboratories, Gaithersburg, Maryland). Thereafter, the plate was washed 3 times with PBS/0.25% Tween 20, and the reaction stopped by tap water, the plate air dried, and the spots were then read. The mean number of spots from triplicate wells was then calculated for each animal. The data were expressed as the mean number of spots per 10^6 PBMC.

2.10. Quantification of plasma viral RNA loads

Virion-associated SHIV RNA loads in the plasma were measured by real-time reverse transcription (RT)-PCR assay [39]. Briefly, total RNA was prepared from the plasma (140 μl) of each macaque with a QIAamp Viral RNA kit (QIAGEN, Hilden, Germany). RT reactions and PCR were performed by a Platinum qRT-PCR ThermoScript One-Step System (Invitrogen, Carlsbad, CA) using the following primers for the gag region: SIV2-696F (5′-GGA AAT TAC CCA GTA CAA CAA ATAGG-3′), and SIV2-784R (5′-TCT ATC AAT TTT ACC CAGGCA TTT A-3′). A labeled probe, SIV2-731T (5′-Fam-TGTCCA CCT GCC ATT AAG CCC G-Tamra-3′), was used for the detection of the PCR products. These reactions were performed with a Prism 7700 Sequence Detector (Applied Biosystems, Foster City, CA) and analyzed using the manufacturer's software. For each run, a standard curve was generated from dilutions whose copy numbers were known, and the RNA in the plasma samples was quantified based on the standard curve. Under these conditions, the detection limit was 1000 copies/ml.

2.11. Flow cytometric analysis

The frequency of $CD4^+$ T lymphocytes in the whole blood was examined by flow cytometry. Blood samples were immunostained with anti-CD3 (FN-18-FITC; Bio Source, Camarillo, CA), anti-CD4 (L200-APC; Becton-Dickinson, Franklin Lakes, NJ), anti-CD8 (SK1-PerCP; Becton-Dickinson), anti-CD28 (CD28.2-PE;

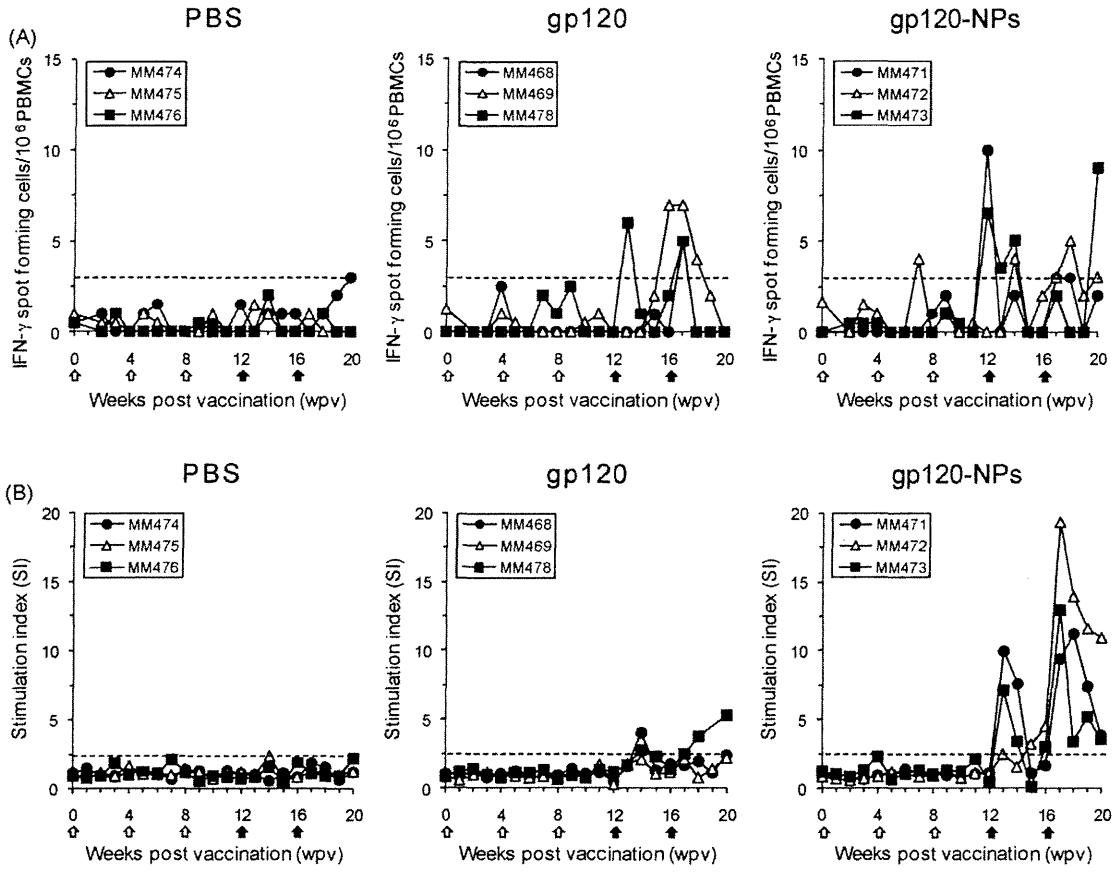

Fig. 1. gp120-specific (A) IFN-γ ELISPOT responses and (B) proliferation responses in PBMCs from macaques immunized with gp120-NPs, gp120-alone and PBS control. The PBMCs from immunized macaques were collected at an interval of 1-week. The results of three individual macaques per group are shown. The white arrows indicate the times of intranasal immunization, and the black arrows indicate the times of subcutaneous immunization. (A) The number of IFN-γ secreting PBMCs detected by ELISPOT after stimulation with gp120. The data represent the mean number of spots per million cells detected in duplicate cultures, after subtracting the mean number of spots found in duplicate control cultures of PBMCs in medium alone. (B) The proliferation of the PBMCs was measured by Brd-U uptake after stimulation with gp120, and is expressed as the stimulation index (SI), as described in Section 2. The cut off value was 2.5 for the SI.

Coulter-Immunotec) and anti-CD95 (DX2-FITC; Becton-Dickinson) antibodies. After hemolysis of the whole blood using FACS™ Lysing Solution (BD PhorMingen, San Diego, CA), each labeled lymphocyte was analyzed on a FACScalibur™ (Becton-Dickinson). The blood was assayed with an automated blood cell counter (F-820; Sysmex, Kobe, Japan).

3. Results

3.1. Vaccination of macaques with gp120-NPs

It is known that gp120-NPs induced efficient cellular immune responses after only one single intranasal immunization in mice [36]. At the beginning, we expected that the gp120-NPs would induce an immune response by very few vaccinations. Nine macaques were intranasally immunized with gp120-NPs (MM471, MM472 and MM473: gp120-NP group), gp120-alone (MM468, MM469 and MM478: gp120-alone group) or PBS as naive controls (MM474, MM475 and MM476: PBS group). However, all macaques had to be subcutaneously immunized twice with additional vaccinations, because their immune responses were insufficient after 3 intranasal immunizations.

To examine whether HIV-1 gp120-specific cellular immunity was induced in the vaccinated macaques, the number of gp120-specific spot forming cells (SFCs) secreting IFN-γ of PBMCs in each macaque group were measured by an ELISPOT assay (Fig. 1A). In all macaques from the PBS group, less than 3 gp120-specific SFC spots were detected throughout the measurement period. On the other hand, in all macaques from the gp120-alone and gp120-NP groups, more than 5 spots of gp120-specific SFCs were detected. The increase of gp120-specific SFCs in the gp120-NP group was earlier than in the gp120-alone group.

Next, we measured the antigen specific proliferation activities by determining the ratio of Brd-U incorporated by PBMCs in the presence of HIV-1 gp120 (Fig. 1B). In the PBS group, gp120-specific proliferation activities were not detected during the measurement period (stimulation index: SI < 2.5). Furthermore, in the gp120-alone and gp120-NP groups, no significant proliferative responses were detected throughout the intranasal immunization period. But after subcutaneous immunization in the gp120-alone and gp120-NP groups, an increase in the activities (SI > 2.5) was detected. Higher proliferative responses were observed in all macaques from the gp120-NP group than in the gp120-alone group.

To examine whether gp120-specific humoral immunities were induced in the vaccinated macaques, we measured anti-gp120-specific antibody levels in the plasma with the ELISA method (Fig. 2). Although, plasma anti-gp120-specific IgG and IgA antibodies were non-specifically detected at higher levels in one macaque from the PBS group (MM476), no significant increase in titer was observed in PBS group throughout the measurement period. Furthermore, in the gp120-alone and gp120-NP groups, no significant increase in titer was detected throughout the intranasal immunization period except for the plasma anti-gp120 IgG antibodies from one macaque (MM469) in the gp120-alone group. After subcutaneous immunization, in all macaques from the gp120-alone and gp120-NP groups, both plasma anti-gp120 IgG and IgA antibodies

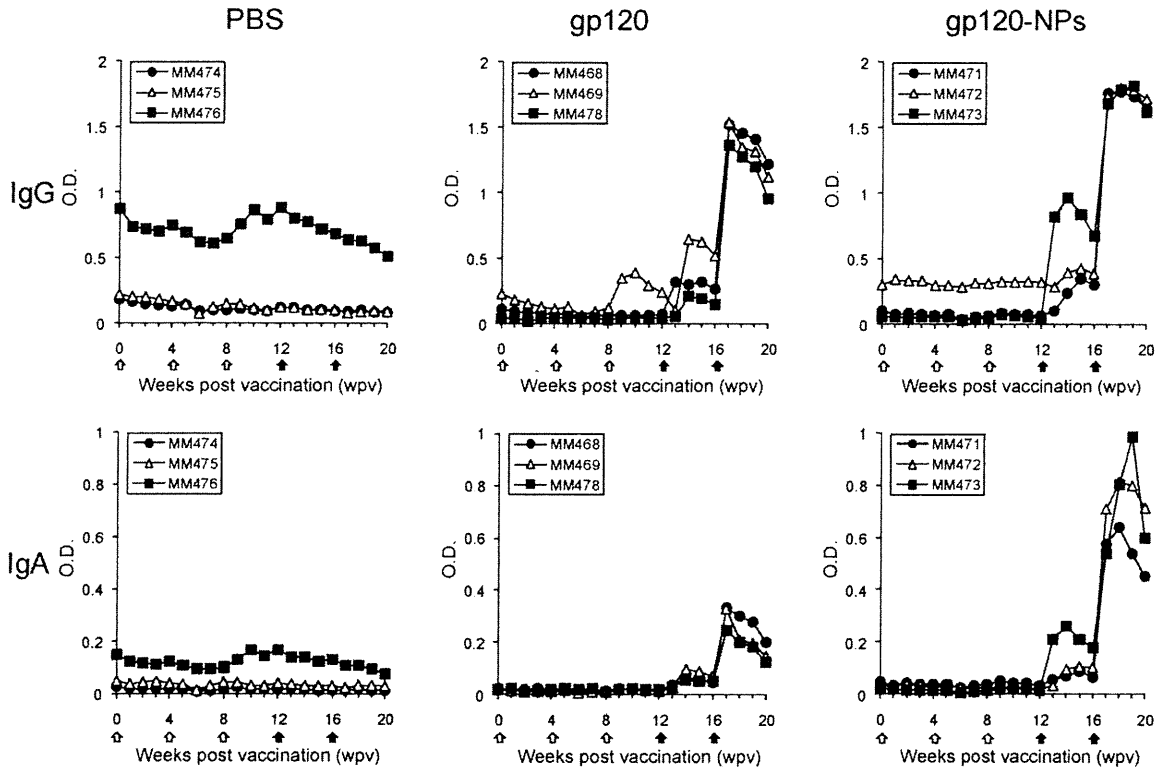

Fig. 2. Anti-HIV-1 gp120 IgG and IgA antibody levels in the plasma of macaques immunized with gp120-NPs, gp120-alone and PBS control. Plasma samples were collected at an interval of 1-week. The levels of gp120-specific IgG and IgA antibodies were measured by ELISA. Plasma samples were assayed after 100-fold dilution. The data are expressed as the optical density (O.D.). The white arrows indicate the times of intranasal immunization, and the black arrows indicate the times of subcutaneous immunization.

were clearly increased. A higher titer was detected in all macaques from the gp120-NP group than in the gp120-alone group. Thus, additional subcutaneous immunizations of 300 μg of gp120 antigen induced clear immune responses in the macaques, although the first 3 bouts of intranasal immunizations with 100 μg of gp120 antigen were insufficient. The induced cellular and humoral immune responses were higher in the gp120-NP group than in the gp120-alone group.

3.2. Intravenous challenge of the vaccinated macaques with SHIV-KU-2

To evaluate the protective effects provided by immunization with gp120-NP, a pathogenic virus, SHIV-KU-2, was intravenously challenged to vaccinated macaques 4 weeks after the last immunization. The plasma viral RNA load and $CD4^+$ T cell counts in the peripheral blood were then monitored.

The plasma viral RNA load in two macaques from the PBS group (MM474 and 475) increased with a peak of 10^6–10^7 copies/ml at 1-week post challenge (wpc), and one macaque (MM476) showed over 10^8 copies/ml after 2 wpc. Then, the viral load in all macaques decreased to below the 10^4 copies/ml after 10 wpc (Fig. 3). On the other hand, in all macaques from the gp120-alone and gp120-NP groups, the viral RNA load peaked at over 10^8 copies/ml at 2 wpc. Furthermore, two of the three macaques in the gp120-NP group (MM472 and 473) showed over 10^6 copies/ml after 10 wpc, although the viral RNA load of the other macaques decreased to below 10^5 copies/ml at those time points. Thus, the challenged virus had replicated more in the vaccinated groups than in the PBS control group. Furthermore, this tendency was more intense in the gp120-NP group than in the gp120-alone group.

The number of $CD4^+$ T cells in the peripheral blood of all macaques in the gp120-alone and gp120-NP groups decreased drastically to below 20% of the pre-challenge levels by 3 wpc, although the $CD4^+$ T cells were not so severely decreased in two of the three macaques in the PBS control group (MM474 and 475) (Fig. 4A). Thereafter, in two macaques from the gp120-NP group (MM472 and MM473) and one macaque from the gp120-alone group (MM469) remained below 20% of the pre-challenge levels until 12 wpc, according to the results of the plasma viral RNA load. Thus, the $CD4^+$ T cells in the peripheral blood were more severely decreased in the vaccinated groups than in the PBS control group. Furthermore, this tendency was more pronounce in the gp120-NP group than in the gp120-alone group.

To understand the decrease in the $CD4^+$ T cell population in the peripheral blood in more detail, we analyzed the $CD4^+$ T cell subpopulations using a CD95 marker. In two of the three macaques from the PBS group (MM474 and MM475), the $CD95^-$ naive $CD4^+$ T cell subpopulation remained over 30% after challenge (Fig. 4B). On the other hand, in all macaques from the gp120-alone and gp120-NP groups and one macaque from the PBS group (MM476), the naive $CD4^+$ T cell subpopulation decreased to below 20%. In all macaques, the $CD95^+$ memory $CD4^+$ T cell subpopulation transiently increased at 1 wpc and thereafter, in most of the macaques, it was maintained at the pre-challenge levels (20–40%) except for two macaques from the gp120-NP group (MM472 and MM473). The memory $CD4^+$ T cell population of these macaques decreased to below 10% after 3 wpc, and did not recover until 12 wpc (data not shown). Thus, in those macaques who showed a high viral load and severe $CD4^+$ T cell depletion, the memory $CD4^+$ T cell subpopulation was more severely injured as compared to the other macaques.

3.3. Virus-specific immune responses after the challenge infection of SHIV-KU-2

To assess the systemic immune responses in vaccinated macaques after the intravenous challenge infection, the virus-specific antibody levels in the plasma of macaques challenged

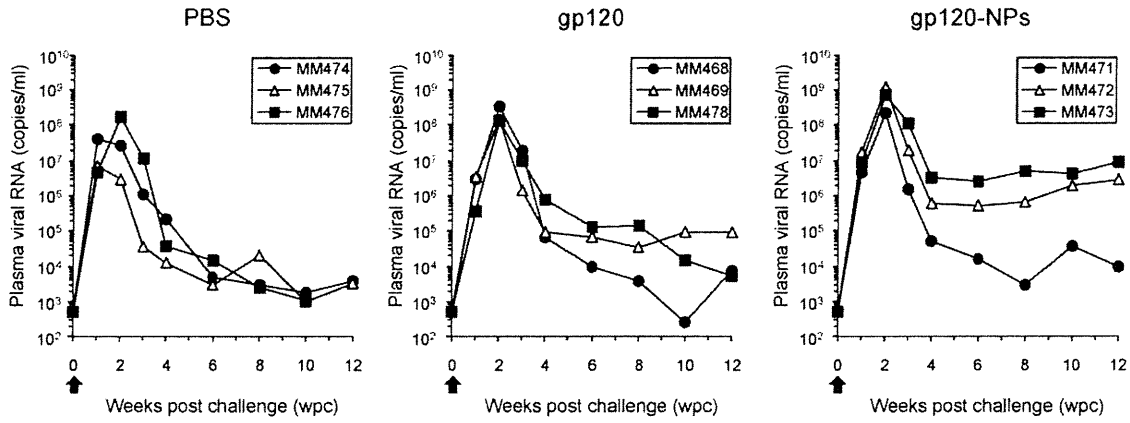

Fig. 3. Plasma viral RNA loads in the peripheral blood of SHIV-KU-2 infected macaques after intravenous inoculation with SHIV-KU-2. The unimmunized (PBS) and immunized (gp120-alone and gp120-NPs) macaques were intravenously challenged with SHIV-KU-2. The plasma viral RNA loads were measured by RT-PCR with a detection limit of 5×10^2 copies/ml. The black arrows indicate the time of challenge with SHIV-KU-2.

with SHIV-KU-2 were measured by the particle agglutination test (Table 1). In the gp120-alone and gp120-NP groups, the initial antibody responses were delayed as compared to the PBS group. In particular, MM472 and MM473 of the gp120-NP group had high viral loads, and the antibody titers were also low in these macaques. These results suggest that there was no protective effect against SHIV-KU-2 in both gp120-NP and gp120-alone groups, in contrast to the immunization-increased viral proliferation.

To assess the effects of the immunization, the lymphocyte proliferation activities after SHIV-KU-2challenge were measured by determining the ratio of Brd-U incorporated by PBMCs in the presence of HIV-1 gp120 and SIV p27 (Fig. 5). First, the gp120-specific lymphocyte proliferation activities were increased in two macaques from the PBS group at 2, 4 (MM476) and 8 wpc (MM475). In two macaques from the gp120-alone group (MM468 and MM469), an increase in proliferative activities could be detected at 2 and 3 wpc. On the other hand, in three macaques from the gp120-NP group, an increase in proliferative responses was observed after 1 wpc (MM472 and MM473) and 2 wpc (MM471). In other words, the increase in activity in the gp120-NP group could be detected earlier than any other group. p27-specific lymphocyte proliferation activities were increased in three macaques from the PBS group at 2 wpc (MM475 and MM476) and 3 wpc (MM474). After 4 wpc in the PBS group, higher proliferative responses were observed in

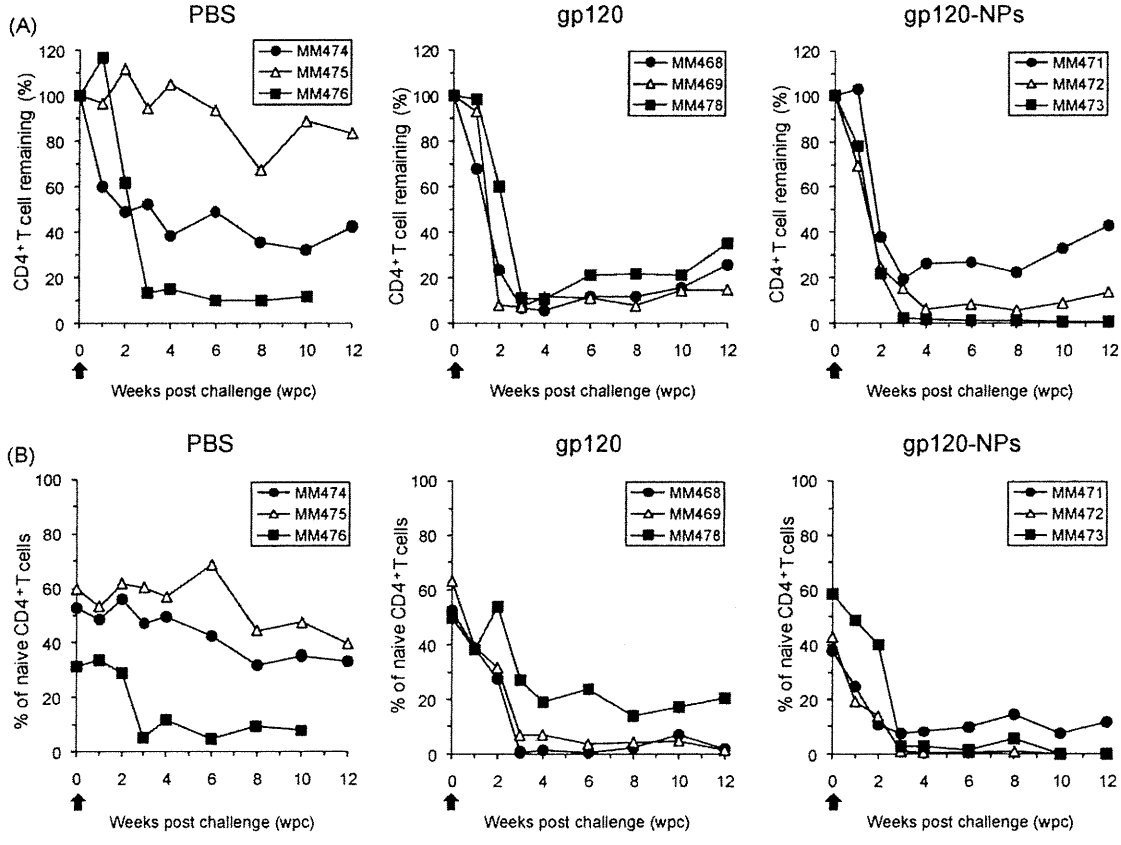

Fig. 4. The number of (A) $CD4^+$ T cells and (B) $CD95^-$ naive $CD4^+$ T cells in the peripheral blood of SHIV-KU-2 infected macaques after an intravenous inoculation with SHIV-KU-2. (A) The number of $CD4^+$ T cells was determined by flow cytometry. The data are expressed as a percent of the cell counts immediately before challenge. (B) Sequential changes in the proportion of the subpopulation (CD95 negative naive cells) of the peripheral blood $CD4^+$ T cells. The percentage of these cells in the $CD4^+$ T cells was determined by flow cytometry. The black arrows indicate the time of challenge with SHIV-KU-2.

Table 1
HIV-1/2 specific antibody responses in the plasma obtained from vaccinated macaques after the intravenous SHIV-KU-2 challenge.

Groups	Macaques	Weeks post challenge (wpc)							
		1	2	3	4	6	8	10	12
PBS	MM474	n.d.	4096	>16,384	>16,384	>16,384	>16,384	>16,384	>16,384
	MM475	n.d.	4096	>16,384	>16,384	>16,384	>16,384	>16,384	>16,384
	MM476	n.d.	8192	>16,384	>16,384	>16,384	>16,384	>16,384	–
gp120	MM468	n.d.	1024	1024	4096	>16,384	>16,384	>16,384	>16,384
	MM469	n.d.	4096	>16,384	>16,384	>16,384	>16,384	>16,384	>16,384
	MM478	n.d.	256	512	8192	>16,384	>16,384	>16,384	>16,384
gp120-NPs	MM471	n.d.	4096	>16,384	>16,384	>16,384	>16,384	>16,384	>16,384
	MM472	32	4096	4096	2048	>16,384	8192	4096	2048
	MM473	n.d.	1024	1024	256	512	512	256	128

Antibodies to HIV *gag* p24 and *env* gp41 in the plasma were measured by the PA method. The data indicated as the titer of serial dilution. n.d.: not detected.

all macaques. In all macaques from the gp120-alone group, the increase in activity could be detected after 2 wpc. On the other hand, in only one macaque from the gp120-NP group (MM471) with a low viral load, an increase in activity was observed after 3 wpc. In the gp120-NP and gp120-alone groups, an increased plasma viral RNA load, and a reduction in $CD4^+$ T cells in the peripheral blood, and gp120-specific lymphocyte proliferation were identified at 1–3 wpc. However, in the PBS group, p27-specific lymphocyte proliferation was identified at the same time, and was higher than in the immunized group after 4 wpc. These results suggest that immunization with gp120-NPs or gp120-alone enhanced gp120-specific immunity, but immunity to the gp120 antigen did not become effective against viral infection or viral proliferation.

4. Discussion

Polymeric nanoparticles have been investigated as an efficient delivery system to APCs for a protein antigen [40]. Therefore biodegradable NPs consisting of γ-PGA derived from *Bacillus* represent a system with efficient immune induction [41–48] and safety [45,46], since it is specifically taken up by dedicated APCs such as DCs [34,44], and is easily disintegrated by proteases [49]. In immune induction experiments using mice with HIV-1 *env*-gp120 carrying γ-hPGA NPs (gp120-NPs), it was shown that both cellular and humoral immune responses were efficiently induced by a low number of vaccinations, suggesting the possibility of use as an efficient vaccine candidate for HIV-1 infection [36]. However, it is unknown whether the immune responses induced in the mouse have protective effects against HIV infection, because HIV-1 is not contagious to mice. Therefore, we immunized rhesus macaques with gp120-NPs in this study to clarify the immune induction capabilities of gp120-NPs and their protective effects against viral infection using a SHIV infection system, because this could not be confirmed with the mouse model.

In the mouse experiments, potent specific cellular immunity was induced with a single intranasal administration of gp120-NPs

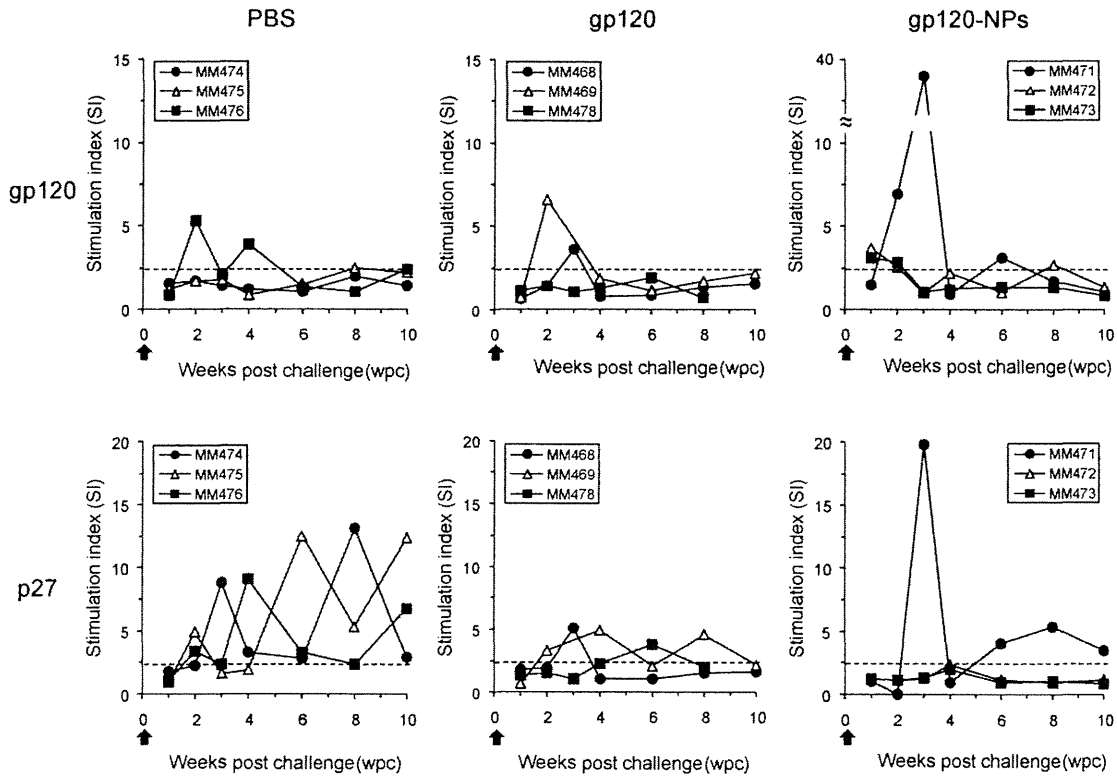

Fig. 5. Antigen-specific lymphocyte proliferation responses in PBMCs from macaques challenged with SHIV-KU-2. The proliferation of the PBMCs was measured by Brd-U uptake after stimulation with gp120 or p27, and was expressed as a stimulation index (SI) as described in Section 2. The cut off value is 2.5 for the SI. The arrows indicate the time of challenge with SHIV-KU-2.

[36]. It has also been reported that mucosal immunization with an HIV-1 vaccine can induce mucosal and systemic HIV-1-specific humoral and cellular immune responses in macaques [20,50,51]. Therefore, we selected intranasal immunization as the administration route of vaccines. However, we determined that three intranasal administrations with 100 μg of gp120-NPs were not able to induce a sufficient immune response in the macaques. Therefore, we performed two additional subcutaneous administrations with 300 μg of gp120-NPs. In this experiment, 100 μg of gp120 was used for each nasal administration. This quantity was decided by a calculation from the optimal amount per weight obtained from mouse experiments. Other research groups administered it intramuscularly or subcutaneously, with more amount of gp120, and obtained antigen-specific cellular immunity and antibody responses [52,53], although they used a different antigen delivery system. In our particulate delivery system, a greater amount of antigen was necessary to induce a specific immune response in macaques than in mice. An additional two subcutaneous administrations with 300 μg of gp120-NPs induced not only cellular immune responses, but also humoral antibody responses (IgG and IgA), which was poorly induced in the mouse experiments [35], indicating a boost effect in macaques. After the subcutaneous immunization, the increase in gp120-specific IFN-γ producing cells, the increase in gp120-specific cell proliferation activity and the anti-gp120 antibody titer (IgG and IgA) in the plasma were confirmed in all macaques immunized with gp120-NPs and gp120-alone. In both cellular and humoral immune responses, the degree of immune induction was clearly stronger in the gp120-NP immunized macaques than in the gp120-alone immunized macaques. Thus, it became clear that γ-hPGA NPs had an immune reinforcement effect not only in the mice, but also in the rhesus macaques. However, the numbers of gp120-specific SFCs in the gp120-NP group obtained from ELISPT assay were low at less than 10 spots per million PBMCs. These results suggest that antigen-specific CD8 T cell responses were not or poorly induced by the vaccination of gp120-NPs. Consequently, CD4 T cell responses were primarily enhanced in macaques immunized with gp120-NPs.

To examine the protective effects of the gp120-specific immune responses induced by gp120-NPs against viral infection, a challenge inoculation with pathogenic SHIV-KU2 was performed in immunized macaques. Against our expectations, no protective effect was observed. Instead, a promotion of viral growth was observed in immunized macaques as compared to naive control macaques. Furthermore, the degree of reinforcement of the infection was stronger in the gp120-NP immunized macaques than in the gp120-alone immunized macaques. The gp120-specific immune responses induced by vaccination correlated with the promotion of viral growth in between groups. However, there was no definite the correlation between the immune responses and viral road of within-group. Since the target cells for primate lentivirus infection are immune cells such as $CD4^+$ T cells and macrophages, the only useful immune reaction should be activated protection against viral infection. In other words, there is a case for promoting viral replication by inappropriate or insufficient immune responses. For example, there were some antibodies reinforcing the HIV-1 infection [54,55], and HIV-1 is preferentially contagious to memory $CD4^+$ T cells, which are specific for HIV-1 antigens [56]. In this study, we used gp120 as the antigen based on the result that the immune response against *env* was better than that against *gag* in a mouse study [36,37]. The number of $CD4^+$ T cells in the peripheral blood decreased conspicuously at the same time as the immune response specific for gp120 appeared early after virus inoculation in the gp120-NP and gp120-alone vaccinated groups. On the other hand, in the naive control group, the immune response specific for p27 (*gag*) was detected, but not the immune response specific for gp120 (*env*) early after the virus inoculation. Thus, the $CD4^+$ T cells in the peripheral blood were maintained without any decrease in 2 out of 3 naive control macaques. Recently, it has been reported that the strength of the specific immune response against *gag*, i.e. the internal protein structure of the virus is correlated to the decrease in the quantity of virus in the peripheral blood of HIV-1 infected patients. In contrast, the strength of the specific immune responses against the *env* in the crust protein and accessory proteins are correlated to the increase in the quantity of blood virus [57]. Our result that the vaccination of rhesus macaques inducing a specific immune response against *env*-gp120 showed an enhancement of viral replication was consistent with the observations in HIV-1 infected patients, supporting the importance of antigen selection for HIV-1 vaccine development. Moreover, some groups have recently argued that activated $CD4^+$ T cells induced by vaccination in macaques can be an attractive target for SIV infection [58,59]. It is likely that the macaques immunized with gp120-NPs were primarily enhanced gp120-specific CD4 T cell responses but not CD8 T cell. The balance of CD4 and CD8 T cell mediated responses induced by vaccination may be critical in determining viral exclusion and replication.

The total picture of the immune system which is truly important for infection control in individuals infected with the AIDS virus is not yet clarified, and the further accumulation of basic information about the immune correlates for protective immunity is necessary. In our previous project, the partial protective effects of viral replication was obtained in vaccinated macaques by using different nanoparticles connecting the inactivated whole virus particles, not a refined protein [28]. The whole virion is considered to include many kinds of antigens acting for infection restraint and/or promotion. It may be possible to induce only effective immune responses acting for infection restraint with a biodegradable nanoparticle vaccine, distinguishing the restraint-related and promotion-related antigens by a detailed examination of the antigen enclosed in the γ-hPGA NPs in the future. Although cell-mediated immunity against peptide epitopes of viral structural proteins is the mainstream for vaccine development research, other poorly analyzed target antigens such as glycolipids, lipoproteins and nuclear antigens may also have to be examined.

In this study, it was demonstrated that biodegradable nanoparticles composed of amphiphilic γ-PGA have a reinforcement effect for immune responses, and have an impact on important immune cell populations participating in viral replication in infected individuals, although the result was the opposite to our expectation. It is important to ascertain the correct antigen stimulation to guide the patient's immunity to act on infection defense and viral replication restraint effectively using a primate experimental infection model. These biodegradable nanoparticles are expected to be useful as an antigen delivery tool in AIDS vaccine development research.

Acknowledgment

This work was supported by CREST from the Japan Science and Technology Agency (JST).

References

[1] Letvin NL. Correlates of immune protection and the development of a human immunodeficiency virus vaccine. Immunity 2007;27:366–9.
[2] Pomerantz RJ, Horn DL. Twenty years of therapy for HIV-1 infection. Nat Med 2003;9:867–73.
[3] Chun TW, Fauci AS. Latent reservoirs of HIV: obstacles to the eradication of virus. Proc Natl Acad Sci USA 1999;96:10958–61.
[4] Zhao Z, Leong KW. Controlled delivery of antigens and adjuvants in vaccine development. J Pharm Sci 1996;85:1261–70.
[5] Singh M, O'Hagan D. Advances in vaccine adjuvants. Nat Biotechnol 1999;17:1075–81.
[6] Storni T, Kundig TM, Senti G, Johansen P. Immunity in response to particulate antigen-delivery systems. Adv Drug Deliv Rev 2005;57:333–55.
[7] Greenland JR, Letvin NL. Chemical adjuvants for plasmid DNA vaccines. Vaccine 2007;25:3731–41.

[8] O'Hagan DT, Lavelle E. Novel adjuvants and delivery systems for HIV vaccines. AIDS 2002;16:115–24.
[9] Reddy ST, Swartz MA, Hubbell JA. Targeting dendritic cells with biomaterials: developing the next generation of vaccines. Trends Immunol 2006;27:573–9.
[10] Waeckerle-Men Y, Groettrup M. PLGA microspheres for improved antigen delivery to dendritic cells as cellular vaccines. Adv Drug Deliv Rev 2005;57:475–82.
[11] Shibata R, Igarashi T, Haigwood N, Buckler-White A, Ogert R, Ross W, et al. Neutralizing antibody directed against the HIV-1 envelope glycoprotein can completely block HIV-1/SIV chimeric virus infections of macaque monkeys. Nat Med 1999;5:204–10.
[12] Mascola JR, Stiegler G, VanCott TC, Katinger H, Carpenter CB, Hanson CE, et al. Protection of macaques against vaginal transmission of a pathogenic HIV-1/SIV chimeric virus by passive infusion of neutralizing antibodies. Nat Med 2000;6:207–10.
[13] Parren PW, Marx PA, Hessell AJ, Luckay A, Harouse J, Cheng-Mayer C, et al. Antibody protects macaques against vaginal challenge with a pathogenic R5 simian/human immunodeficiency virus at serum levels giving complete neutralization in vitro. J Virol 2001;75:8340–7.
[14] Borrow P, Lewicki H, Hahn BH, Shaw GM, Oldstone MB. Virus-specific CD8+ cytotoxic T-lymphocyte activity associated with control of viremia in primary human immunodeficiency virus type 1 infection. J Virol 1994;68:6103–10.
[15] Ogg GS, Jin X, Bonhoeffer S, Dunbar PR, Nowak MA, Monard S, et al. Quantitation of HIV-1-specific cytotoxic T lymphocytes and plasma load of viral RNA. Science 1998;279:2103–6.
[16] Matano T, Shibata R, Siemon C, Connors M, Lane HC, Martin MA. Administration of an anti-CD8 monoclonal antibody interferes with the clearance of chimeric simian/human immunodeficiency virus during primary infections of rhesus macaques. J Virol 1998;72:164–9.
[17] Schmitz JE, Kuroda MJ, Santra S, Sasseville VG, Simon MA, Lifton MA, et al. Control of viremia in simian immunodeficiency virus infection by CD8+ lymphocytes. Science 1999;283:857–60.
[18] McMichael AJ, Hanke T. HIV vaccines 1983–2003. Nat Med 2003;9:874–80.
[19] Verschoor EJ, Mooij P, Oostermeijer H, van der Kolk M, ten Haaft P, Verstrepen B, et al. Comparison of immunity generated by nucleic acid-MF59-, and ISCOM-formulated human immunodeficiency virus type 1 vaccines in Rhesus macaques: evidence for viral clearance. J Virol 1999;73:3292–300.
[20] Yoshino N, Lu FX, Fujihashi K, Hagiwara Y, Kataoka K, Lu D, et al. A novel adjuvant for mucosal immunity to HIV-1 gp120 in nonhuman primates. J Immunol 2004;173:6850–7.
[21] Koopman G, Bogers WM, van Gils M, Koornstra W, Barnett S, Morein B, et al. Comparison of intranasal with targeted lymph node immunization using PR8-Flu ISCOM adjuvanted HIV antigens in macaques. J Med Virol 2007;79:474–82.
[22] Barnett SW, Srivastava IK, Kan E, Zhou F, Goodsell A, Cristillo AD, et al. Protection of macaques against vaginal SHIV challenge by systemic or mucosal and systemic vaccinations with HIV-envelope. AIDS 2008;22:339–48.
[23] Flynn NM, Forthal DN, Harro CD, Judson FN, Mayer KH, Para MF, et al. Placebo-controlled phase 3 trial of a recombinant glycoprotein 120 vaccine to prevent HIV-1 infection. J Infect Dis 2005;191:654–65.
[24] Bogers WM, Cheng-Mayer C, Montelaro RC. Developments in preclinical AIDS vaccine efficacy models. AIDS 2000;14:141–51.
[25] Akagi T, Kawamura M, Ueno M, Hiraishi K, Adachi M, Serizawa T, et al. Mucosal immunization with inactivated HIV-1-capturing nanospheres induces a significant HIV-1-specific vaginal antibody response in mice. J Med Virol 2003;69:163–72.
[26] Akagi T, Ueno M, Hiraishi K, Baba M, Akashi M. AIDS vaccine: intranasal immunization using inactivated HIV-1-capturing core-corona type polymeric nanospheres. J Control Release 2005;109:49–61.
[27] Wang X, Akagi T, Akashi M, Baba M. Development of core-corona type polymeric nanoparticles as an anti-HIV-1 vaccine. Mini-Rev Org Chem 2007;4:281–90.
[28] Miyake A, Akagi T, Enose Y, Ueno M, Kawamura M, Horiuchi R, et al. Induction of HIV-specific antibody response and protection against vaginal SHIV transmission by intranasal immunization with inactivated SHIV-capturing nanospheres in macaques. J Med Virol 2004;73:368–77.
[29] Akagi T, Baba M, Akashi M. Preparation of nanoparticles by the self-organization of polymers consisting of hydrophobic and hydrophilic segments: potential applications. Polymer 2007;48:6729–47.
[30] Matsusaki M, Hiwatari K, Higashi M, Kaneko T, Akashi M. Stably-dispersed and surface-functional bionanoparticles prepared by self-assembling amphipathic polymers of hydrophilic poly(γ-glutamic acid) bearing hydrophobic amino acids. Chem Lett 2004;33:398–9.
[31] Akagi T, Kaneko T, Kida T, Akashi M. Preparation and characterization of biodegradable nanoparticles based on poly(γ-glutamic acid) with L-phenylalanine as a protein carrier. J Control Release 2005;108:226–36.
[32] Akagi T, Kaneko T, Kida T, Akashi M. Multifunctional conjugation of proteins on/into core-shell type nanoparticles prepared by amphiphilic poly(γ-glutamic acid). J Biomater Sci Polym Ed 2006;17:875–92.
[33] Kim H, Akagi T, Akashi M. Preparation of size tunable amphiphilic poly(amino acid) nanoparticles. Macromol Biosci 2009;9:842–8.
[34] Uto T, Wang X, Sato K, Haraguchi M, Akagi T, Akashi M, et al. Targeting of antigen to dendritic cells with poly(γ-glutamic acid) nanoparticles induces antigen-specific humoral and cellular immunity. J Immunol 2007;178:2979–86.
[35] Akagi T, Wang X, Uto T, Baba M, Akashi M. Protein direct delivery to dendritic cells using nanoparticles based on amphiphilic poly(amino acid) derivatives. Biomaterials 2007;28:3427–36.
[36] Wang X, Uto T, Akagi T, Akashi M, Baba M. Induction of potent CD8+ T-cell responses by novel biodegradable nanoparticles carrying human immunodeficiency virus type 1 gp120. J Virol 2007;81:10009–16.
[37] Wang X, Uto T, Akagi T, Akashi M, Baba M. Poly(γ-glutamic acid) nanoparticles as an efficient antigen delivery and adjuvant system: potential for an AIDS vaccine. J Med Virol 2008;80:11–9.
[38] Joag SV, Li Z, Foresman L, Stephens EB, Zhao LJ, Adany I, et al. Chimeric simian/human immunodeficiency virus that causes progressive loss of CD4+ T cells and AIDS in pig-tailed macaques. J Virol 1996;70:3189–97.
[39] Suryanarayana K, Wiltrout TA, Vasquez GM, Hirsch VM, Lifson JD. Plasma SIV RNA viral load determination by real-time quantification of product generation in reverse transcriptase-polymerase chain reaction. AIDS Res Hum Retroviruses 1998;14:183–9.
[40] Peek LJ, Middaugh CR, Berkland C. Nanotechnology in vaccine delivery. Adv Drug Deliv Rev 2008;60:915–28.
[41] Matsuo K, Yoshikawa T, Oda A, Akagi T, Akashi M, Okada N, et al. Efficient generation of antigen-specific cellular immunity by vaccination with poly(γ-glutamic acid) nanoparticles entrapping endoplasmic reticulum-targeted peptides. Biochem Biophys Res Commun 2007;362:1069–72.
[42] Okamoto S, Yoshii H, Akagi T, Akashi M, Ishikawa T, Okuno Y, et al. Influenza hemagglutinin vaccine with poly(γ-glutamic acid) nanoparticles enhances the protection against influenza virus infection through both humoral and cell-mediated immunity. Vaccine 2007;25:8270–8.
[43] Okamoto S, Yoshii H, Ishikawa T, Akagi T, Akashi M, Takahashi M, et al. Single dose of inactivated Japanese encephalitis vaccine with poly(γ-glutamic acid) nanoparticles provides effective protection from Japanese encephalitis virus. Vaccine 2008;26:589–94.
[44] Yoshikawa T, Okada N, Oda A, Matsuo K, Matsuo K, Mukai Y, et al. Development of amphiphilic γ-PGA-nanoparticle based tumor vaccine: potential of the nanoparticulate cytosolic protein delivery carrier. Biochem Biophys Res Commun 2008;366:408–13.
[45] Yoshikawa T, Okada N, Oda A, Matsuo K, Matsuo K, Kayamuro H, et al. Nanoparticles built by self-assembly of amphiphilic poly(γ-glutamic acid) can deliver antigens to antigen-presenting cells with high efficiency: a new tumor-vaccine carrier for eliciting effector T cells. Vaccine 2008;26:1303–13.
[46] Uto T, Wang X, Akagi T, Zenkyu R, Akashi M, Baba M. Improvement of adaptive immunity by antigen-carrying biodegradable nanoparticles. Biochem Biophys Res Commun 2009;379:600–4.
[47] Uto T, Akagi T, Hamasaki T, Akashi M, Baba M. Modulation of innate and adaptive immunity by biodegradable nanoparticles. Immunol Lett 2009;125:46–52.
[48] Okamoto S, Matsuura M, Akagi T, Akashi M, Tanimoto T, Ishikawa T, et al. Poly(γ-glutamic acid) nano-particles combined with mucosal influenza virus hemagglutinin vaccine protects against influenza virus infection in mice. Vaccine 2009;27:5896–905.
[49] Akagi T, Higashi M, Kaneko T, Kida T, Akashi M. Hydrolytic and enzymatic degradation of nanoparticles based on amphiphilic poly(γ-glutamic acid)-*graft*-L-phenylalanine copolymer. Biomacromolecules 2006;7:297–303.
[50] Imaoka K, Miller CJ, Kubota M, McChesney MB, Lohman B, Yamamoto M, et al. Nasal immunization of nonhuman primates with simian immunodeficiency virus p55gag and cholera toxin adjuvant induces Th1/Th2 help for virus-specific immune responses in reproductive tissues. J Immunol 1998;161:5952–8.
[51] Egan MA, Chong SY, Hagen M, Megati S, Schadeck EB, Piacente P, et al. A comparative evaluation of nasal and parenteral vaccine adjuvants to elicit systemic and mucosal HIV-1 peptide-specific humoral immune responses in cynomolgus macaques. Vaccine 2004;22:3774–88.
[52] Mooij P, van der Kolk M, Bogers WM, ten Haaft PJ, Van Der Meide P, Almond N, et al. A clinically relevant HIV-1 subunit vaccine protects rhesus macaques from in vivo passaged simian-human immunodeficiency virus infection. AIDS 1998;12:15–22.
[53] Earl PL, Sugiura W, Montefiori DC, Broder CC, Lee SA, Wild C, et al. Immunogenicity and protective efficacy of oligomeric human immunodeficiency virus type 1 gp140. J Virol 2001;75:645–53.
[54] Robinson Jr WE, Kawamura T, Gorny MK, Lake D, Xu JY, Matsumoto Y, et al. Human monoclonal antibodies to the human immunodeficiency virus type 1 (HIV-1) transmembrane glycoprotein gp41 enhance HIV-1 infection in vitro. Proc Natl Acad Sci USA 1990;87:3185–9.
[55] Takeda A, Robinson JE, Ho DD, Debouck C, Haigwood NL, Ennis FA. Distinction of human immunodeficiency virus type 1 neutralization and infection enhancement by human monoclonal antibodies to glycoprotein 120. J Clin Invest 1992;89:1952–7.
[56] Douek DC, Brenchley JM, Betts MR, Ambrozak DR, Hill BJ, Okamoto Y, et al. HIV preferentially infects HIV-specific CD4+ T cells. Nature 2002;417:95–8.
[57] Kiepiela P, Ngumbela K, Thobakgale C, Ramduth D, Honeyborne I, Moodley E, et al. CD8+ T-cell responses to different HIV proteins have discordant associations with viral load. Nat Med 2007;13:46–53.
[58] Staprans SI, Barry AP, Silvestri G, Safrit JT, Kozyr N, Sumpter B, et al. Enhanced SIV replication and accelerated progression to AIDS in macaques primed to mount a CD4 T cell response to the SIV envelope protein. Proc Natl Acad Sci USA 2004;101:13026–31.
[59] Tsukamoto T, Takeda A, Yamamoto T, Yamamoto H, Kawada M, Matano T. Impact of cytotoxic-T-lymphocyte memory induction without virus-specific CD4+ T-Cell help on control of a simian immunodeficiency virus challenge in rhesus macaques. J Virol 2009;83:9339–46.

Virology 399 (2010) 134–143

Contents lists available at ScienceDirect

Virology

journal homepage: www.elsevier.com/locate/yviro

In vivo analysis of a new R5 tropic SHIV generated from the highly pathogenic SHIV-KS661, a derivative of SHIV-89.6

Kenta Matsuda, Katsuhisa Inaba, Yoshinori Fukazawa, Megumi Matsuyama, Kentaro Ibuki, Mariko Horiike, Naoki Saito, Masanori Hayami, Tatsuhiko Igarashi, Tomoyuki Miura *

Laboratory of Primate Model, Experimental Research Center for Infectious Diseases, Institute for Virus Research, Kyoto University, 53 Shogoinkawaramachi, Sakyo-ku, Kyoto 606-8507, Japan

ARTICLE INFO

Article history:
Received 9 November 2009
Returned to author for revision
14 December 2009
Accepted 5 January 2010
Available online 27 January 2010

Keywords:
AIDS
SHIV
CCR5 tropic
Mutagenesis
V3 region

ABSTRACT

Although X4 tropic SHIVs have been studied extensively, they show distinct infection phenotypes from those of R5 tropic viruses, which play an important role in HIV-1 transmission and pathogenesis. To augment the variety of R5 tropic SHIVs, we generated a new R5 tropic SHIV from the highly pathogenic X4 tropic SHIV-KS661, a derivative of SHIV-89.6. Based on consensus amino acid alignment analyses of subtype B R5 tropic HIV-1, five amino acid substitutions in the third variable region successfully changed the secondary receptor preference from X4 to R5. Improvements in viral replication were observed in infected rhesus macaques after two passages, and reisolated virus was designated SHIV-MK38. SHIV-MK38 maintained R5 tropism through *in vivo* passages and showed robust replication in infected monkeys. Our study clearly demonstrates that a minimal number of amino acid substitutions in the V3 region can alter secondary receptor preference and increase the variety of R5 tropic SHIVs.

Introduction

Simian immunodeficiency virus (SIV) macaque models for AIDS have been used extensively to elucidate the pathogenesis of human immunodeficiency virus type 1 (HIV-1) infection. Although SIV is an excellent model virus that has contributed to various virological discoveries, SIV has many limitations as an HIV-1 model. Because the antigenicity of SIV is different from that of HIV-1, it is difficult to evaluate HIV-1 vaccines in animal models by employing SIV as a challenge virus. This is especially true for evaluating the induction of neutralizing antibodies by HIV-1 vaccine candidates (Baba et al., 2000; Dey et al., 2009; Mascola et al., 2000). In addition to CCR5, SIV utilizes secondary receptors such as GPR1, GPR15 (Bob), and STRL-33 (Bonzo), which are scarcely used by HIV-1 (Clapham and McKnight, 2002). Although there have been no reports that have directly demonstrated the significance of these receptors for *in vivo* pathogenesis, possible influences of these minor receptors cannot be denied.

To supplement the limitations of the SIV model, a simian and human immunodeficiency virus (SHIV) macaque model has been generated. SHIVs were constructed by exchanging the envelope gene and other accessory genes of SIV with that of HIV-1 (Shibata et al., 1991). Therefore, SHIVs share the same envelope antigenicity and receptor usage with HIV-1. In early studies of HIV-1, isolated viruses were mostly X4 or dual tropic because they were isolated from AIDS patients using T-cell lines expressing CXCR4. Because envelope genes from X4 or dual tropic viruses were introduced to generate the chimeric virus, most SHIVs utilize CXCR4 as a secondary receptor. X4 tropic viruses infect distinct subsets of lymphocytes and the mode of viral replication during the acute phase of infection is different from that of R5 tropic viruses (Nishimura et al., 2004). During the acute phase of infection, X4 tropic SHIVs rapidly deplete circulating CD4 positive (+) T cells (Reimann et al., 1996; Sadjadpour et al., 2004). Most infected monkeys fail to seroconvert, because rapid depletion of helper T cells typically occurs within 4 weeks of infection. In contrast, R5 tropic viruses do not show such a catastrophic reduction in CD4+ T cells. The phenotypes observed during X4 SHIV infection are rare during actual HIV-1 infection, and it has been suggested that R5 tropic viruses are mainly involved in HIV-1 transmission and pathogenesis (Margolis and Shattock, 2006). Therefore, there is a demand for R5 tropic SHIVs in this field of research.

There are some R5 tropic SHIVs that have already been used in various experiments, including analyses on the efficacy of broadly neutralizing antibodies (Hessell et al., 2009). Due to the paucity of available R5 tropic SHIVs, however, it is difficult to conduct comparative analyses on the efficacy of neutralizing antibodies between different strains of SHIVs. *In vivo* analyses of neutralizing antibodies should be conducted with more than one or even a mixture of several strains of R5 tropic virus to reflect the wide variety of HIV-1 envelope genes that are found worldwide. Therefore, our primary aim

* Corresponding author. Mailing address: Laboratory of Primate Model, Experimental Research Center for Infectious Diseases, Institute for Virus Research, Kyoto University, 53 Shogoinkawaramachi, Sakyo-ku, Kyoto 606-8507, Japan. Fax: +81 75 761 9335.
E-mail address: tmiura@virus.kyoto-u.ac.jp (T. Miura).

0042-6822/$ – see front matter © 2010 Elsevier Inc. All rights reserved.
doi:10.1016/j.virol.2010.01.008

was to generate a new R5 tropic SHIV, which carries a different *env* from that of other existing R5 SHIVs.

Currently available R5 SHIVs were constructed by introducing the envelope gene and other accessory genes from R5 tropic HIV-1 into the SIV backbone (Humbert et al., 2008; Luciw et al., 1995). There is one report that demonstrated the construction of an R5 tropic SHIV by exchanging the whole third variable region (V3) of an X4 tropic SHIV with that of an R5 SHIV (Ho et al., 2005). This study clearly indicated that the V3 region of the envelope gene determines the secondary receptor preference *in vivo*. Although other studies have indicated that there are specific amino acids within the V3 region that are responsible for receptor preference (Cardozo et al., 2007; Yamaguchi-Kabata et al., 2004), there have been no reports demonstrating the generation of R5 tropic SHIV by the introduction of specific amino acid substitutions to the V3 region. Therefore, our secondary aim in this study was to alter the receptor usage of a well-studied X4 tropic SHIV by introducing a minimal number of amino acid substitutions in the *env* V3 region. The consensus amino acid alignment of subtype B R5 tropic HIV-1, which is strongly correlated with secondary receptor usage (Cardozo et al., 2007; Yamaguchi-Kabata et al., 2004), was introduced to the V3 region of a highly pathogenic SHIV-KS661 that possesses the typical infection phenotype of X4 tropic SHIV (Fukazawa et al., 2008; Miyake et al., 2006). SHIV-KS661 is a molecular clone constructed from the consensus sequence of SHIV-C2/1 (Gen Bank accession number AF21718) (Shinohara et al., 1999), a derivative of the non-pathogenic SHIV-89.6

Results

Generation of R5 tropic SHIV-MK1 from the highly pathogenic X4 tropic SHIV-KS661

The X4 tropic virus SHIV-KS661, a derivative of SHIV-89.6, depletes CD4+ T lymphocytes in systemic tissues within weeks of infection and causes AIDS-like symptoms in macaque monkeys (Fukazawa et al., 2008; Miyake et al., 2006). To convert the virus into an R5 tropic virus, we introduced five amino acid substitutions in the V3 region of SHIV-KS661 by site-directed mutagenesis. The positions of the substitutions were selected using information from alignment of the V3 amino acids of R5 tropic HIV-1 (Cardozo et al., 2007; Yamaguchi-Kabata et al., 2004). All five substitutions (E305K, R306S, R318T, R319G, and N320D) were accompanied by changes in electrical charge. As a result, the net charge of the V3 region shifted towards being more acidic (Fig. 1A). To determine whether this mutant, designated SHIV-MK1, was capable of replication within monkey cells, we spinoculated SHIV-MK1 on rhPBMCs at an MOI of 0.1. The RT activity in the supernatant was monitored daily. The X4 tropic SHIV-DH12R-CL-7 and parental SHIV-KS661 actively replicated on rhPBMCs, reaching its peak RT activity level 4 days after inoculation. The R5 tropic SIVmac239 reached its peak RT value at the same time point; however, the peak value was less than 50% of that of SHIV-DH12R-CL-7 and SHIV-KS661. SHIV-MK1 also replicated on rhPBMCs, but it took 2 days longer to reach peak RT activity levels, and the peak RT value was significantly lower than that of the parental SHIV-KS661 (Fig. 1B).

Next, to determine whether SHIV-MK1 was capable of utilizing CCR5, but not CXCR4, we conducted a small molecule inhibitor assay. Briefly, SIVmac239, SHIV-DH12R-CL-7, SHIV-KS661, or SHIV-MK1 was spinoculated on rhPBMCs that were preincubated with AD101 (R5 inhibitor), AMD3100 (X4 inhibitor), or both inhibitors at various concentrations. The supernatant RT activities were measured 5 days post-inoculation. The replication of X4 tropic SHIV-DH12-CL-7 was inhibited with AMD3100 in a dose-dependent manner; however, it was not restrained with AD101 as described previously (Igarashi et al., 1999, 2003; Sadjadpour et al., 2004). The same pattern was observed in SHIV-KS661-infected rhPBMCs, thus indicating that this virus is also an X4 tropic virus. In contrast, there was no replication inhibition of R5 tropic SIVmac239 in the presence of AMD3100; however, dose-dependent inhibition was observed in the presence of AD101. This result is consistent with other reports (Marcon et al., 1997; Zhang et al., 2000). SHIV-MK1 exhibited the same inhibition profile as SIVmac239, indicating that this virus predominantly utilizes CCR5, but not CXCR4, as an entry secondary receptor.

R5 tropic SHIV-MK1 can replicate in rhesus macaques

To determine whether SHIV-MK1 is capable of replication in rhesus macaques, we intravenously inoculated two monkeys (MM482 and MM483) with 20,000 TCID50 SHIV-MK1. Large amount of virus was inoculated to this group of monkey because *in vitro* replication of SHIV-MK1 was significantly weak compared with that of parental SHIV-KS661. As a control, two other monkeys (MM455 and MM459) were infected with 2000 TCID50 SHIV-KS661, a sufficient amount of virus to induce AIDS-like symptoms (Fukazawa et al., 2008; Miyake et al., 2006). Plasma viral RNA loads were monitored periodically using quantitative RT-PCR. Both groups of infected monkeys exhibited viremia, which reached peak plasma viral RNA loads of 10^6–10^8 copies/ml 2 weeks post-infection. In SHIV-KS661-infected monkeys, the set point of plasma viral RNA loads was between 10^4 and 10^6 copies/ml (Fig. 2Ai). In contrast, the plasma viral RNA load in one of the two monkeys infected with SHIV-MK1 was undetectable by 6 weeks post-infection, although 10-fold more virus was inoculated. The other monkey maintained 10^3–10^4 copies/ml plasma viral RNA for more than 25 weeks post-infection (Fig. 2Aii).

Next, circulating CD4+ T lymphocytes were analyzed by fluorescence activated cell sorting (FACS) to elucidate the impact of infection on lymphocyte subsets. As previously reported, X4 tropic SHIV-KS661 caused a massive depletion of circulating CD4+ T lymphocytes within 4 weeks post-infection (Fig. 2Bi). In contrast, circulating CD4+ T lymphocytes transiently decreased in monkeys infected with SHIV-MK1; however, they tended to recover by 24 weeks post-infection (Fig. 2Bii).

Because X4 tropic viruses preferably target naive CD4+ T lymphocytes, and R5 tropic viruses preferably target memory CD4+ T lymphocytes, circulating memory and naive CD4+ T lymphocytes were analyzed. The ratios of memory and naive CD4+ T cells were monitored 0, 2, 4, and 8 weeks post-SHIV-MK1 infection (Fig. 2C). Consistent with previous reports (Nishimura et al., 2004), X4 tropic SHIV-KS661 preferentially depleted naive T lymphocytes by 2 weeks post-infection. Although there was a subtle reduction in CD4+ T lymphocytes, the ratio of memory and naive CD4+ T lymphocytes did not change in SHIV-MK1-infected monkeys. This result indicates that a reduction in CD4+ T cells during SHIV-MK1 infection was not sufficient to alter the ratio of memory T cells, at least in circulating T lymphocytes.

The intestine is an effecter site where most CD4+ T lymphocytes are memory cells, and is the primary target for R5 tropic viruses (Harouse et al., 1999; Veazey et al., 1998). To elucidate the impact of viral infection in the intestine, tissue samples from the jejunum were obtained periodically and CD4+ T lymphocyte subsets were analyzed (Fig. 2D). As reported previously, CD4+ T lymphocytes of KS661-infected monkeys were depleted by 4 weeks post-infection (Fukazawa et al., 2008; Miyake et al., 2006). Although CD4+ T lymphocyte depletion was observed in one of the SHIV-MK1-infected monkeys (MM482) within 4 weeks post-infection, CD4+ T lymphocytes recovered as plasma viral RNA loads decreased. Another SHIV-MK1 infected monkey (MM483) whose plasma viral RNA load dropped below detectable levels showed only a transient reduction in CD4+ lymphocytes 5 weeks after infection. Taken together, these results suggest that, although the magnitude of jejunal CD4+ T-cell reduction was greater than that of circulating CD4+ T cells, the capability of SHIV-MK1 to cause CD4+ T lymphocyte depletion in the jejunum is not as strong as the parental SHIV-KS661.

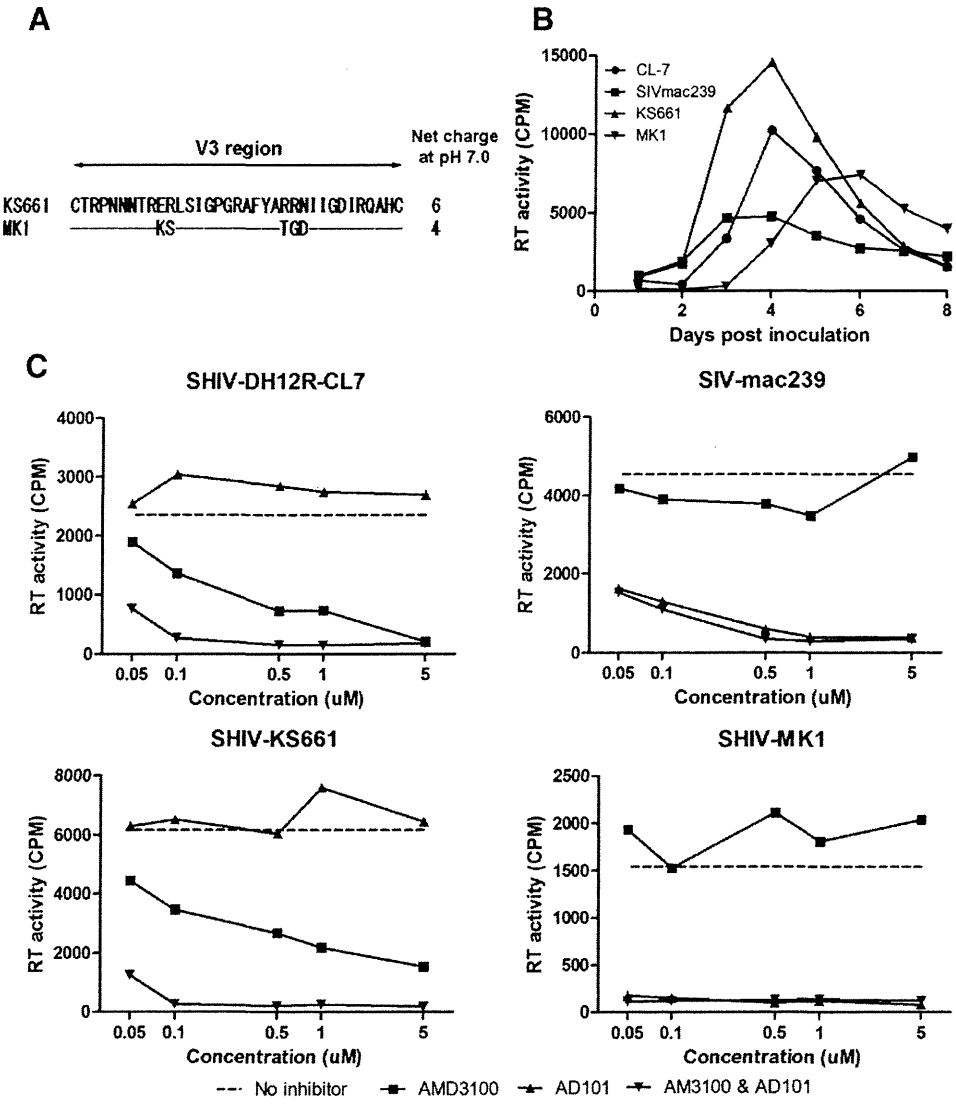

Fig. 1. Construction and *in vitro* analysis of SHIV-MK1. (A) gp120 V3 amino acid alignment of SHIV-MK1. Amino acid substitution positions are indicated under the parental SHIV-KS661 alignment. The net charge at pH 7.0 is indicated beside each amino acid alignment. (B) SHIV and SIV replication in rhPBMCs. The replication of control viruses (SIVmac239, SHIV-DH12R-CL7, and SHIV-KS661) and the mutant virus (SHIV-MK1) are shown. Culture supernatants were collected at the indicated time points, and RT activity was determined. Representative results of three independent experiments are shown. (C) Secondary receptor inhibitor sensitivity of the three SHIV inocula and an SIV control. The inoculum viruses SHIV-DH12R-CL7, SIVmac239, SHIV-KS661, and SHIV-MK1 were spinoculated on rhPBMCs in the presence of the indicated small molecule inhibitors. The inhibitor concentrations used were 0.05, 0.1, 0.5, 1, and 5 μM. The RT activity on day 5 post-infection was determined by the absence (dashed line) or presence of an inhibitor in the medium.

In vivo passage and characterization of the reisolated virus, SHIV-MK38

To adapt SHIV-MK1, we conducted *in vivo* passages. Briefly, disaggregated lymphocytes from inguinal lymph nodes and fresh blood collected from SHIV-MK1-infected MM482, were mixed and intravenously inoculated into an uninfected monkey, MM498. During the first passage, MM498 showed a plasma viral RNA load peak and set point equal to that of SHIV-MK1-infected MM482. During the second passage, disaggregated lymphocytes from inguinal lymph nodes and fresh blood collected from MM498 were mixed and intravenously inoculated into an uninfected monkey, MM504. MM504 showed a peak plasma viral RNA load of 5×10^7 copies/ml, which is slightly higher than that of MM482 and MM498. Furthermore, the set point of the viral load ranged from 10^4 to 10^6 copies/ml, which is approximately 10 times higher than that of MM482 and MM498 (Fig. 3A).

Although the inoculum doses were different in passaged monkeys, this result suggests that SHIV-MK1 acquired a better replicative capacity through *in vivo* passage. Therefore, we decided to reisolate the virus from MM504 for *in vitro* characterization. Briefly, CD8-depleted PBMCs from MM504 and an uninfected monkey were co-cultured for 2 weeks. The culture supernatant with the highest RT activity was stored in liquid nitrogen. This virus stock was designated SHIV-MK38.

First, we examined the replication kinetics of SHIV-MK38 in rhPBMCs. The infection assay revealed that although SHIV-MK38 could not replicate as fast or as efficiently as the parental KS661, there was a slight improvement in replication capacity compared with the original SHIV-MK1 (Fig. 3B). This result indicates that mutations that arose through *in vivo* passage increased replication ability in rhPBMCs.

As shown in Fig. 1B, however, X4 tropic viruses (SHIV-DH12R-CL-7 and SHIV-KS661) usually show fast and efficient replication in PBMCs compared with that of R5 tropic viruses (SIVmac239 and SHIV-MK1). Hence, there is the possibility of reversion in the V3 region, which may give SHIV-MK38 the appearance of having better replication capacity in rhPBMCs (Cho et al., 1998). Therefore, we examined the viral genome sequence to rule out the presence of reversions in the V3 region. Indeed, there were no back mutations in the V3 region of SHIV-MK38 when the V1 to V3 regions of the *env* sequences from 14

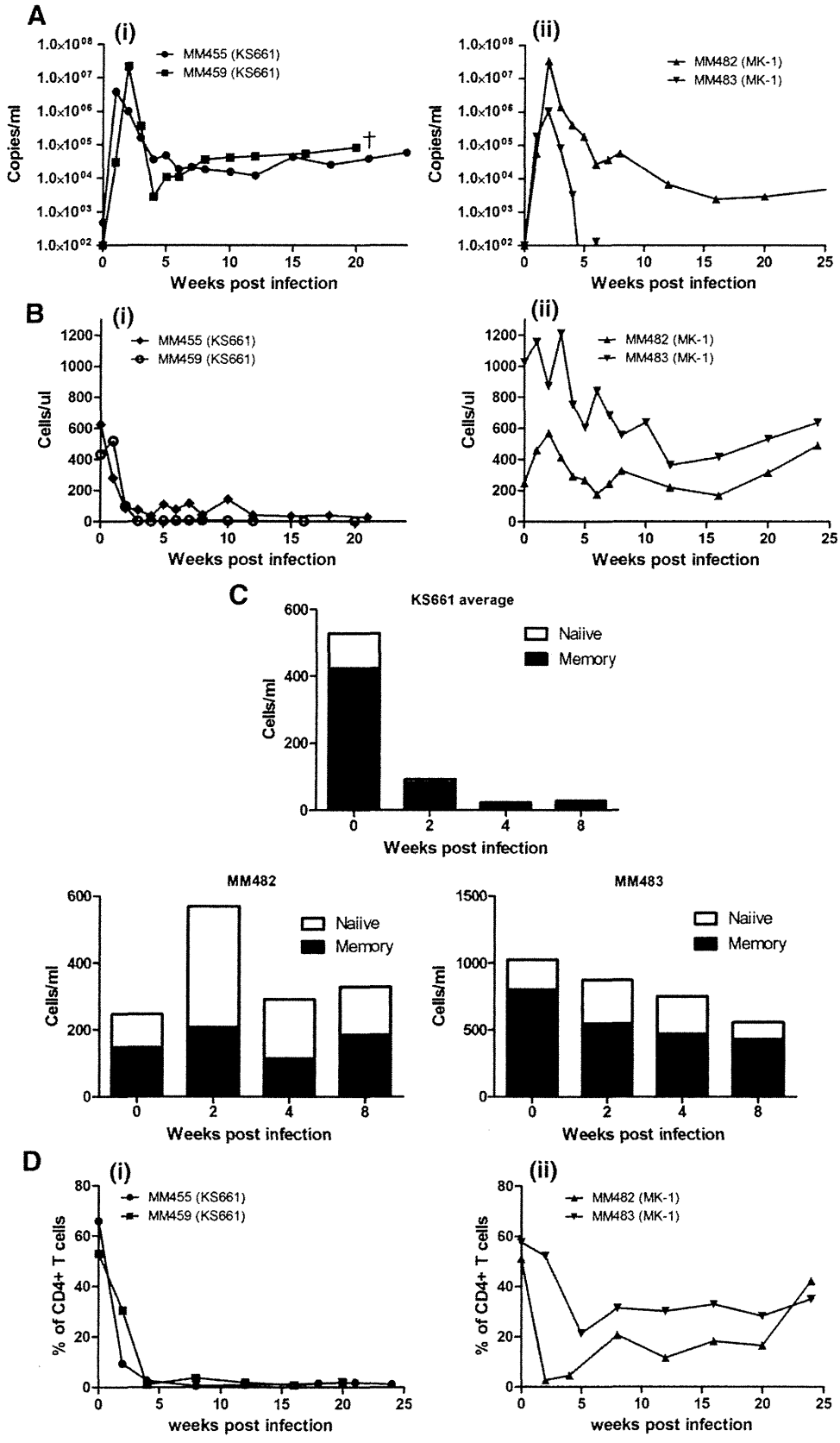

Fig. 2. *In vivo* replication of MK1. (A) Plasma viral RNA loads in SHIV-infected rhesus monkeys were measured at the indicated times. A total of 2000 TCID50 SHIV-KS661 was inoculated intravenously into MM455 and MM459 as a control group (i) and 20,000 TCID50 SHIV-MK1 was inoculated intravenously into MM482 and MM483 (ii). (B) CD4+ T lymphocytes were enumerated using FACS analysis in the SHIV-KS661 infected group (i) and the SHIV-MK1 infected group (ii) over the course of infection. (C) Changes in naive (open bar) and memory (black bar) CD4+ T cells in rhesus macaques inoculated with SHIV-KS661 (average of two infected monkeys) and SHIV-MK1 (MM482 and MM483) 0, 2, 4, and 8 weeks post-inoculation. (D) Percentage of CD4+ T lymphocytes in the jejunum. Tissues from the jejunum were collected from SHIV-KS661 infected monkeys (i) and SHIV-MK1 infected monkeys (ii) with a pediatric enteroscope, and were analyzed by FACS.

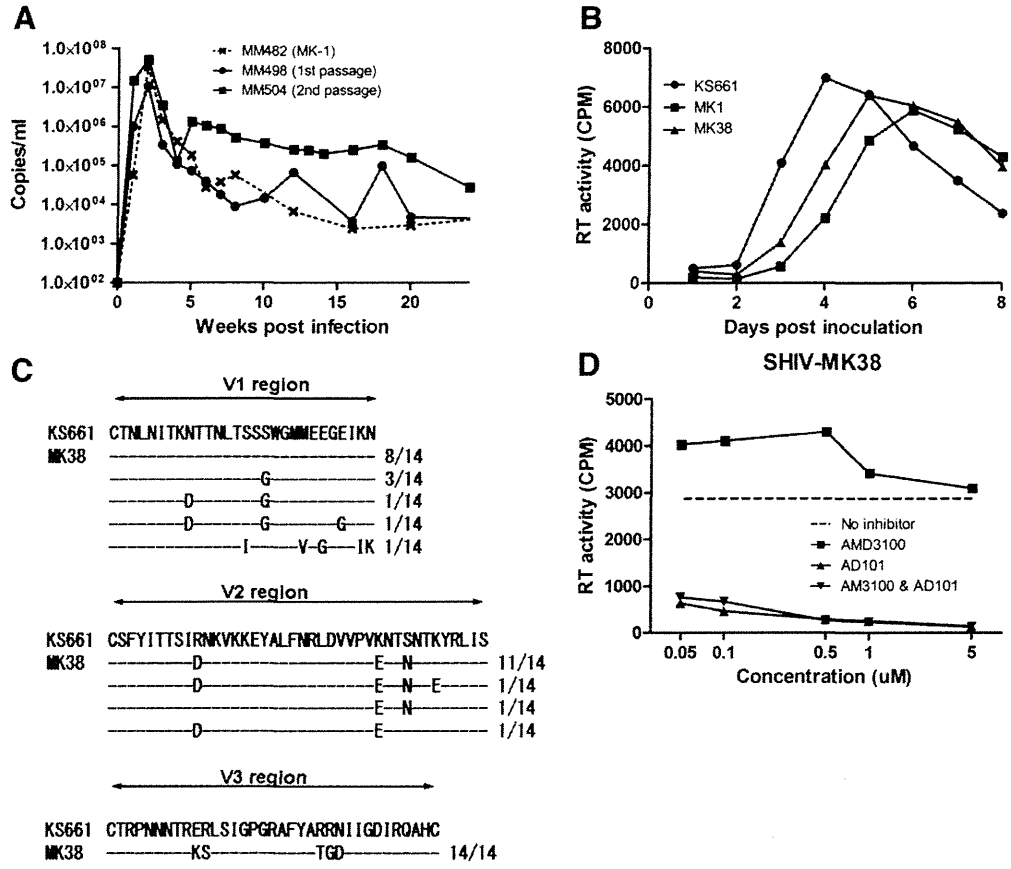

Fig. 3. *In vivo* adaptation of SHIV-MK1, and *in vitro* analysis of reisolated virus. (A) Plasma viral RNA loads of passaged monkeys were measured at the indicated times. The whole blood and dissociated lymph nodes from SHIV-MK1-infected MM482 were transfused into MM498 (first passage) 25 weeks post-inoculation. The whole blood and disaggregated lymph nodes from MM498 were transfused into MM504 (second passage) 5 weeks post-inoculation. (B) SHIV replication in rhPBMCs. The replication of control viruses (SHIV-KS661 and SHIV-MK1) and a passaged virus (SHIV-MK38) is shown. Culture supernatants were collected at the indicated time points, and RT activity was determined. Representative results of three independent experiments are shown. (C) gp120 V1, V2, and V3 amino acid alignment of SHIV-KS661 and 14 clones of SHIV-MK38. The positions of the amino acid substitutions in the 14 clones are indicated under the SHIV-KS661 sequence. (D) Secondary receptor inhibitor sensitivity of the SHIV-MK38 inoculum. RT activity 5 days post-infection was determined in the absence (dashed line) or presence of an inhibitor in the medium.

clones were analyzed (Fig. 3C). Nonetheless, we found mutations in the V1 and V2 regions of SHIV-MK38. These mutations have the potential to affect secondary receptor usage.

To confirm whether SHIV-MK38 maintains R5 tropism, we conducted a small molecule inhibitor assay, which revealed that SHIV-MK38 could not replicate in rhPBMCs in the presence of AD101 but could replicate in the presence of AMD3100. This indicates that SHIV-MK38 maintains R5 tropism in the primary cell (Fig. 3D).

In vivo analysis of SHIV-MK38

To evaluate whether SHIV-MK38-infected monkeys show stable infection phenotypes compared with that of SHIV-MK1-infected monkeys, we inoculated three monkeys with 20,000 TCID50 SHIV-MK38. All three infected monkeys possessed a peak plasma viral RNA load of approximately 10^7 copies/ml 12 days after infection. Although the peak plasma viral RNA load was at the same level in these monkeys, set points varied widely (Fig. 4A). That of MM501 was 10^3–10^4 copies/ml, which is similar to that of SHIV-MK1-infected MM482. MM502 had a slightly higher set point of 10^4–10^5 copies/ml, which is similar to that of MM504. Finally, MM481 had the highest set point, at 10^6–10^7 copies/ml. No monkey showed a decrease in viral RNA load under the detectable level, indicating that SHIV-MK38 robustly replicates in rhesus macaques.

Next, reductions in circulating CD4+ T cells were analyzed. Unlike SHIV-MK1 infection, all of the SHIV-MK38-infected monkeys exhibited a continuous reduction in CD4+ T cells without signs of recovery (Fig. 4B). The impact of infection on ratios of circulating memory and naive CD4+ T cells was also analyzed. Compared with monkeys infected with SHIV-MK1, SHIV-MK38 preferentially reduced memory fractions of CD4+ T cells (Figs. 2C and 4C).

To elucidate how improvements in viral replication affect the reduction of CD4+ T cells at effector sites, tissue samples from the jejunum were obtained periodically and CD4+ T lymphocyte subsets were analyzed. In SHIV-MK38-infected monkeys, CD4+ T cells were rapidly reduced by 2 weeks post-infection, as seen in SHIV-MK1 infection. Furthermore, recovery of CD4+ T cells was not observed in infected monkeys. In particular, CD4+ T cells in MM481 were depleted throughout the observation period (Figs. 2D and 4D). These data indicate that SHIV-MK38 has an increased ability to reduce CD4+ T cells and maintain higher plasma viral RNA loads in infected monkeys compared with pre-adapted SHIV-MK1.

Discussion

Based on the analysis of consensus amino acid alignments of subtype B R5 viruses, five amino acid substitutions (E305K, R306S, R318T, R319G, and N320D) were introduced into the V3 region of the pathogenic SHIV-KS661 *env* gene by site-directed mutagenesis. These substitutions included the 11/24/25th amino acid of the V3 region, which are strongly correlated with secondary receptor usage (Cardozo et al., 2007; Yamaguchi-Kabata et al., 2004). As expected, these substitutions successfully altered the secondary receptor usage of SHIV-KS661 from X4 to R5 tropic. This result clearly demonstrates

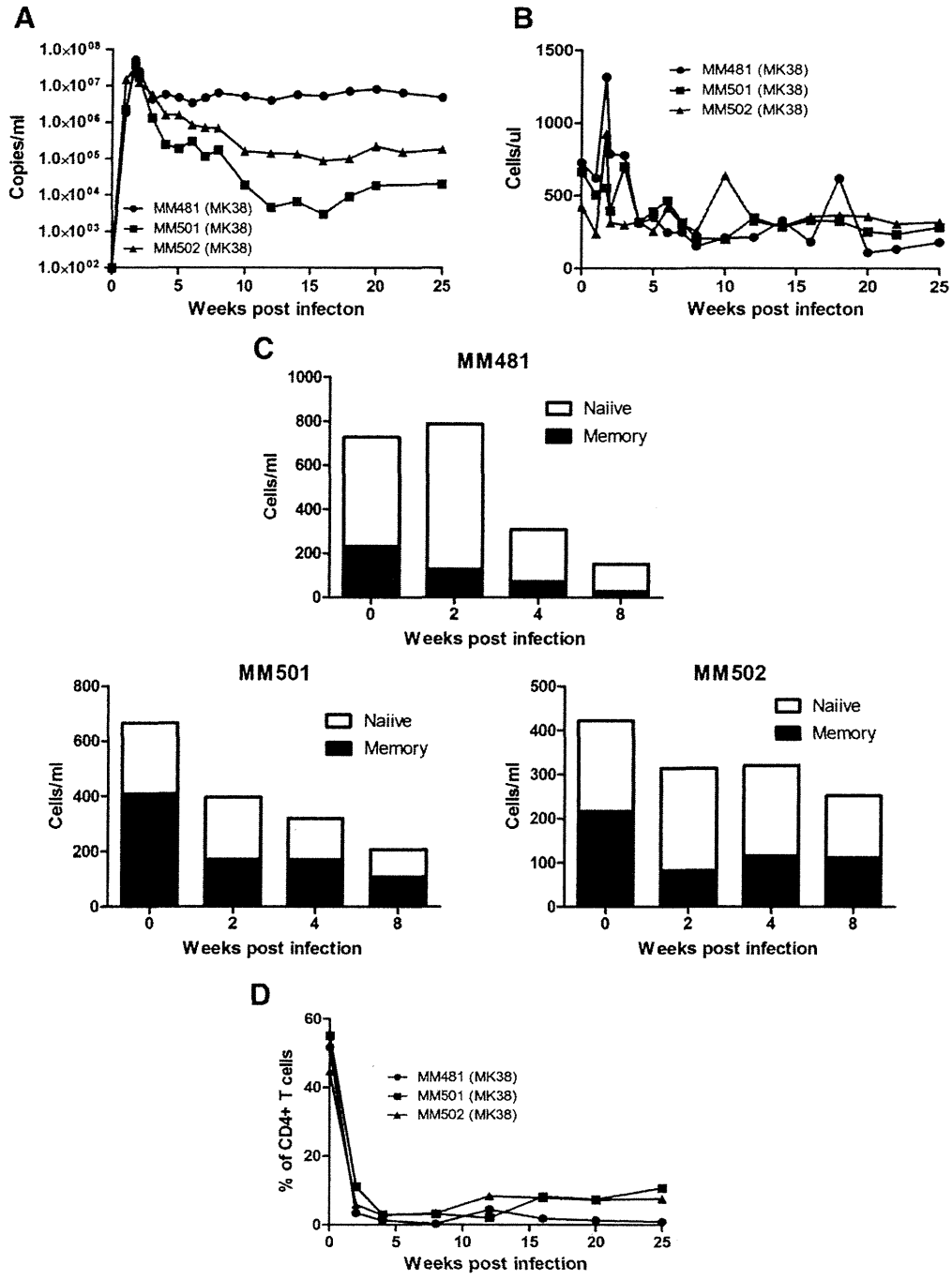

Fig. 4. *In vivo* replication of SHIV-MK38. (A) Plasma viral RNA loads in SHIV-infected rhesus monkeys were measured at the indicated times. A total of 20,000 TCID50 SHIV-MK38 were inoculated into MM481, MM501, and MM502. (B) CD4+ T lymphocytes were enumerated using FACS analysis in SHIV-MK38-infected monkeys over the course of infection. (C) Changes in naïve (open bar) and memory (filled bar) CD4+ T cells in rhesus macaques inoculated with SHIV-MK38 0, 2, 4, and 8 weeks post-inoculation. (D) Percentage of CD4+ T lymphocytes in the jejunum. Tissues from the jejunum were collected from SHIV-MK38-infected monkeys with a pediatric enteroscope, and analyzed by FACS.

for the first time that specific V3 amino acid alignment information from HIV-1 can be applied to SHIV to alter secondary receptor usage, at least in the context of the subtype B envelope. The prediction of viral secondary receptor tropism in HIV-1-infected people prior to the prescription of CCR5 antagonists has important economic and practical implications. There are at least six algorithms that predict viral tropism from the V3 sequence; however, the accuracy of these algorithms must be improved (de Mendoza et al., 2008; Dorr et al., 2005; Fätkenheuer et al., 2005; Mefford et al., 2008). For example, the Web PSSM algorithm (Jensen et al., 2003) predicts that SHIV-MK1 exclusively utilizes CCR5, while the Geno2pheno algorithm (Sing et al., 2007) suggests that it may also utilize CXCR4. In this study, we demonstrated that specific amino acids in the V3 region are responsible for secondary receptor usage both *in vitro* and *in vivo*. Accumulation of this type of information will provide important data that can be used to improve predictions and increase the genotype sensitivity of algorithms.

Although minimal numbers of amino acid substitutions were introduced to change secondary receptor usage, SHIV-MK1 showed relatively inefficient replication compared with that of parental SHIV-KS661, both *in vitro* and *in vivo*. SHIV-MK1 caused measurable levels of viremia in infected monkeys; however, plasma viral RNA levels dropped below detectable levels in one of two infected monkeys 6 weeks after inoculation, despite the fact that enormous amount of

virus was inoculated. When evaluating the efficacy of passively administered neutralizing antibodies, or those induced by candidate anti-HIV-1 vaccines, this variability in viral replication is not desirable for the assessment of efficacy, because it is impossible to determine whether the virus was controlled by natural immune responses or by vaccine-induced immune responses. However, an improvement in viral replication was observed in rhPBMCs after *in vivo* passage of SHIV-MK1. This outcome suggests that, as in the case of other existing R5 tropic SHIVs, *in vivo* adaptation is required regardless of the minimal number of amino acid substitutions (Humbert et al., 2008; Tan et al., 1999).

Because various reports have demonstrated the emergence of the X4 tropic virus from the R5 tropic virus after serial passages (Ho et al., 2007; Pastore et al., 2000), there was a concern over the emergence of the X4 tropic virus through two *in vivo* passages. Although there were only five amino acid substitutions, no reversions in any of the substituted amino acids in the V3 region were observed. Some mutations were accompanied by amino acid substitutions in V1 and V2 regions. Previous reports suggest that these two variable regions may influence secondary receptor preference (Cho et al., 1998); however, a small molecule inhibitor assay revealed that SHIV-MK38 maintained R5 tropism after passage. The V1 and V2 regions also play a role in sensitivity against neutralizing antibodies (Laird et al., 2008; Wei et al., 2003). Although further investigations are required, SHIV-MK38 could have developed mutations in the V1 and V2 regions to modify antigenicity in an attempt to evade neutralizing antibodies (Sagar et al., 2006). Indeed, neutralization assay on TZM-BL cells revealed that neutralizing antibody from an MK1-infected monkey can neutralize SHIV-KS661 and SHIV-MK1, but fail to neutralize SHIV-MK38. On the other hand, plasma from the monkey in which SHIV-MK38 was isolated could neutralize all three viruses. Thus, the antigenicity was changed through *in vivo* passages (Supplementary Figure). Taken together, these results suggest that the improved replication of SHIV-MK38 over MK1 was not due to the re-emergence of X4 tropic viruses. Furthermore, the acquisition of mutations outside the V3 region is most likely attributable to the improved replication of SHIV-MK38 *in vivo*.

To confirm the replication advantage of SHIV-MK38 over SHIV-MK1, SHIV-MK38 was intravenously inoculated into three uninfected monkeys. Despite the fact that the same amount of SHIV-MK38 was inoculated, higher peaks and set points of plasma RNA loads were observed in SHIV-MK38 compared with SHIV-MK1 infection. Although SHIV-MK38-infected monkeys showed no obvious signs of AIDS-like symptoms during the observation period, none of these monkeys was able to control viral replication. A greater reduction in the memory portion of circulating CD4+ T cells was observed in SHIV-MK38-infected monkeys. This preferential reduction of circulating memory CD4+ T cells was well defined in MM481, which correlates with the maintenance of high plasma viral RNA loads throughout the observation period. Reductions of CD4+ T cells in the jejunum of SHIV-MK38-infected monkeys were greater than that of SHIV-MK1-infected monkeys, and there was no obvious recovery during the observation period. These infection phenotypes are characteristic of an R5 tropic virus, which is distinct from the infection of X4 tropic SHIVs such as parental SHIV-KS661 (Fukazawa et al., 2008; Miyake et al., 2006).

Harous et al. clearly demonstrated that R5 tropic virus preferentially reduces mucosal CD4+ T cells where memory CD4+ T cells are abundant, whereas X4 tropic virus preferentially reduces peripheral CD4+ T cells where naive CD4+ T cells are abundant (Harouse et al., 1999). From this observation, it is clear that the receptor preference has strong impact on tissue specific CD4+ T-cell reductions. However, in some cases, systemic and irreversible reduction of CD4+ T cells was observed in highly pathogenic X4 SHIV infection (Fukazawa et al., 2008; Nishimura et al., 2004). It has been suggested that highly pathogenic X4 SHIV preferentially targets naive CD4+ T cells but eventually reduces memory CD4+ T cells (Nishimura et al., 2004). The depletion of CD4+ T cells at the effector site in SHIV-KS661 infected monkeys supports this suggestion (Fig. 2D).

The envelope gene of SHIV-MK38 belongs to subtype B, which can be compared with other subtype B or C R5 tropic SHIVs (Humbert et al., 2008; Tan et al., 1999). Comparing the efficacy of passively administered neutralizing antibodies and their induction by candidate HIV-1 vaccines against a variety of R5 tropic SHIVs would provide a more precise evaluation against a variety of HIV-1 strains worldwide (Wei et al., 2003). Furthermore, despite the fact that SHIV-MK38 is derived from SHIV-KS661, and mutations were obtained through the alteration of secondary receptor usage and passage, SHIV-MK38 is still genetically homologous to SHIV-89.6P, because they both originate from the same molecular clone, SHIV-89.6. Highly pathogenic X4 tropic SHIV-89.6P has been used extensively in various experiments, including vaccine concept evaluations (Shiver et al., 2002). There are claims, however, that the utilization of X4 tropic SHIVs as challenge viruses has led to overestimation of vector-based vaccines (Feinberg and Moore, 2002). Therefore, SHIV-MK38 can be useful in the future to determine whether such overestimations are truly caused by using X4 SHIVs or are due to using an SHIV derived from the specific lineage of SHIV-89.6.

Based on our observations, it can be concluded that R5 tropic SHIV-MK38 can robustly replicate, and we successfully generated a new R5 tropic SHIV by a new method. Although infected monkeys showed no signs of AIDS-like symptoms during the observation period, and further characterization such as neutralization profiles must be conducted, SHIV-MK38 has the potential to be a new R5 SHIV model.

Materials and methods

Virus production

Non-synonymous nucleotide substitutions in the V3 domain of the SHIV-KS661 *env* gene were introduced by site-directed mutagenesis for substitution of amino acids. A 5.9 kb DNA fragment containing the *env* V3 domain was subcloned into a pUC119 vector following digestion with restriction enzymes Sse8387I and XhoI. The resulting vector was designated pKS661v3, and was used as the template for two sets of polymerase chain reaction (PCR). All amplifications were performed as follows: one cycle of denaturation (98 °C, 5 min), 32 cycles of amplification (98 °C, 10 s/60 °C, 30 s/72 °C, 2 min), and an additional cycle for final extension (72 °C, 10 min) using iProof High-Fidelity Master Mix (Bio-Rad Laboratories, Hercules, CA). The following primers were used for the first set of PCR: 5′ CAATACAAGAAAAAGTTTATCTATAGGACCAGGGAGAGCATTTTATGCAACAGGAGACATAATAGGAG 3′ (forward primer corresponding to the 7250–7317th nucleotides of SHIV-KS661; positions of mismatches are underlined) and 5′ GCTGAAGAGGCACAGGCTCCGC 3′ (reverse primer corresponding to the 8633–8612th nucleotide of SHIV-KS661; no mismatches). The following primers were used for the second set of PCR: 5′ CTCCTATTATGTCTCCTGTTGCATAAAATGCTCTCCCTGGTCCTATAGATAAACTTTTTCTTGTATTG 3′ (reverse primer corresponding to the 7317–7250th nucleotide of SHIV-KS661; positions of mismatches are underlined) and 5′ CTCCAGGACTAGCATAAATGG 3′ (forward primer corresponding to the 5617–5637th nucleotide of SHIV-KS661; no mismatches). The products from these two sets of PCR were mixed, and overlap PCR was performed using primers 5′ GCTGAAGAGGCACAGGCTCCGC 3′ and 5′ CTCCAGGACTAGCATAAATGG 3′. The PCR product was then digested with the restriction enzymes BsaBI and NcoI. The resulting fragment was introduced back into the pKS661v3 vector, and designated pKS661v3m. Then pKS661v3m DNA with mutations was digested by Sse8387I and XhoI, and the fragment was introduced back into the KS661 full genome plasmid, and designated pMK1.

SHIV-MK1 was prepared by transfecting pMK1 into the 293T cell line using the FuGENE 6 Transfection Reagent (Roche Diagnostics, Indianapolis, IN) and the culture supernatant 48 h after transfection, and was stored in liquid nitrogen until use. The same procedures were conducted to prepare SIVmac239 (Kestler et al., 1991), SHIV-KS661 (Shinohara et al., 1999), and SHIV-DH12R-CL7 (Igarashi et al., 1999). The 50% tissue culture infectious dose (TCID50) was measured using the C8166-CCR5 cell line (Shimizu et al., 2006).

Viral replication on rhPBMCs

Rhesus macaque PBMCs (rhPBMCs), prepared from an uninfected monkey, were suspended in Rosewell Park Memorial Institute (RPMI) 1640 medium supplemented with 10% (vol/vol) fetal bovine serum (FBS), 2 mM L-glutamine, and 1 mM sodium pyruvate, and then stimulated for 20 h with 25 μg/ml Concanavalin A (Sigma-Aldrich, St. Louis, USA), followed by an additional 2-day cultivation with 100 units/ml IL-2 (Shionogi, Osaka, Japan). On day 3, 5×10^4 cells were dispensed into 96-well round-bottom plates in triplicate. The cells were then inoculated with virus at a multiplicity of infection (MOI) of 0.1 using the spinoculation method (O'Doherty et al., 2000). Virion-associated reverse transcriptase (RT) activity of the culture supernatant was monitored periodically (Willey et al., 1988).

Inhibition of viral replication by a small molecule inhibitor

A small molecule inhibitor assay was conducted as described previously (Igarashi et al., 2003), with minor modifications. Briefly, uninfected rhesus PBMCs were prepared as described above. On day 3, 5×10^4 cells were dispensed into 96-well round-bottom plates. Various concentrations (0, 0.05, 0.1, 0.5, 1, and 5 μM) of a small molecule CCR5-specific receptor antagonist (AD101 was provided by Dr. Julie Strizki, Schering Plough Research Institute, Kenilworth, NJ) (Trkola et al., 2002) and/or a CXCR4-specific receptor antagonist (AMD3100; Sigma-Aldrich, St. Louis, MO) (Donzella et al., 1998) were added to duplicate wells and incubated for 1 h at 37 °C. Then each test virus was spinoculated at $1200\times g$ for 1 h at an MOI of 0.1. On day 5 post-infection, virus replications were assessed by RT assay of the culture supernatants.

Virus inoculation

Indian-origin rhesus macaques were used in accordance with the institutional regulations approved by the Committee for Experimental Use of Nonhuman Primates of the Institute for Virus Research, Kyoto University, Kyoto, Japan. Monkeys were housed in a biosafety level 3 facility and all procedures were performed in this facility. Collection of blood, biopsies, and i.v. virus inoculations (2000 TCID50 of SHIV-KS661, 20000 TCID50 of SHIV-MK1, 20000 TCID50 of SHIV-MK38) were performed on monkeys under anesthetization with ketamine hydrochloride (Daiichi-Sankyo, Tokyo, Japan). Plasma viral RNA loads were determined by quantitative RT-PCR as described previously (Kozyrev et al., 2002). Plasma viral RNA loads under 100 copies/ml were characterized as undetectable levels.

Jejunal biopsy

Tissue samples from the jejunum were collected with a pediatric enteroscope (Olympus GIF type XP260N, Olympus Medical System Corp., Tokyo, Japan). Five pieces (samples) of fresh jejunal tissue were placed on a shaker for 2 h at room temperature in 40 ml RPMI 1640 medium containing 10% FBS and 0.01 g collagenase from *Clostridium histolyticum* (Sigma-Aldrich, St. Louis, MO). Disaggregated cells were filtered through glass wool loaded in a 20 ml disposable syringe. Cells were prepared from the filtrate by centrifugation at a speed of 1200 rpm for 10 min. Subsets of lymphocytes in the resuspended cells were analyzed by flow cytometry.

Flow cytometry

To analyze CD4+ T lymphocytes, whole blood and jejunal samples were stained with two fluorescently labeled mouse monoclonal antibodies, fluorescein isothiocyanate (FITC) conjugated anti-monkey CD3 (Clone FN-18, BioSource Intl, Camarillo, CA) and phycoerythrin (PE) conjugated anti-human CD4 (Clone Nu-TH/I; Nichirei, Tokyo, Japan). To analyze memory and naive CD4+ T lymphocytes, whole blood and jejunal samples were stained with three fluorescently labeled mouse monoclonal antibodies, FITC conjugated anti-human CD95 (Clone DX2; BD Pharmingen, Tokyo, Japan), PE conjugated anti-human CD28 (Clone CD28.2; Coulter Immunotech, Marseille, France), and allophycocyanin (APC) conjugated anti-human CD4 (Clone L200; BD Pharmingen). After hemolysis of whole blood and jejunal samples using a lysing solution (Beckton Dickinson, Franklin Lakes, NJ), each type of labeled lymphocyte was examined on a FACScalibur analyzer using Cellquest (BD Biosciences, San Jose, CA). CD95+CD4^{high}+ cells were considered memory T lymphocytes, and CD95-CD28+CD4^{high}+ cells were considered naive T lymphocytes (Pitcher et al., 2002). The absolute number of lymphocytes in the blood was determined using an automated blood counter, KX-21 (Sysmex, Kobe, Japan).

In vivo passage

Inguinal lymph nodes were aseptically collected from MM482 25 weeks after infection. The lymph nodes were minced with scissors, disaggregated using an 85-ml Bellco Tissue Sieve Kit (Bellco Glass, Inc., Vineland, NJ), and filtered through a 100-μm pore cell strainer (REF 35-2360, BD Falcon, Franklin Lakes, NJ). Filtrates were centrifuged and then washed four times with phosphate-buffered saline (PBS). These disaggregated cells were mixed with 2 ml frozen plasma (collected from the animal 8 weeks post-infection and stored at −80 °C) and 20 ml fresh blood from MM482, and then transfused into an uninfected monkey (MM498) intravenously. During the second passage, inguinal lymph nodes were aseptically collected from MM498 5 weeks after infection. The disaggregated inguinal lymph node was mixed with 2 ml frozen plasma (collected 2 weeks post-infection), 5×10^7 cells inguinal lymphocytes (collected 16 days post-infection and stored at −80 °C), and 15 ml fresh blood, and then transfused into an uninfected monkey (MM504).

Reisolation of virus

Fresh blood was obtained from the uninfected monkey, and PBMCs were isolated. These cells were incubated for 30 min with PE labeled anti-CD8 antibody (SK1 clone, BD Pharmingen), then washed once with PBS. Next, cells were incubated with anti-PE MACS beads (Miltenyi Biotec, Bergisch Gladbach, Germany), and CD8− cells were negatively selected with a magnetic column. CD8− PBMCs were cultured as described above.

On day 0, fresh blood was obtained from MM504 (16 weeks post-infection) and CD8 cells were depleted as described above. CD8+ cells were also depleted from frozen PBMCs (obtained from MM504 8 weeks post-infection and stored at −80 °C). These CD8− PBMCs from uninfected and infected monkeys were co-cultured in PBMC culture medium (described above) at a concentration of 2×10^6 cells/ml at 37 °C. Medium was replaced daily for 16 days and culture supernatants were stored at −80 °C. The culture supernatant with the highest RT value was stored in liquid nitrogen. This virus stock was designated SHIV-MK38.